PilT and PilU are homohexameric ATPases that coordinate to retract type IVa pili

Jennifer L. Chlebek[1], Hannah Q. Hughes[1], Aleksandra S. Ratkiewicz[2], Rasman Rayyan[2], Joseph Che-Yen Wang[3], Brittany E. Herrin[1], Triana N. Dalia[1], Nicolas Biais[2], and Ankur B. Dalia[1,*]

[1]Department of Biology, Indiana University, 1001 E. 3rd Street, Bloomington, IN 47405.

[2]Biology Department, CUNY Brooklyn College, 2900 Bedford Avenue, Brooklyn, NY 11210 and Graduate Center of CUNY, 365 5th Avenue, NY 10016.

[3]Electron Microscopy Center, Indiana University, Bloomington, IN 47405.

*Correspondence to: ankdalia@indiana.edu.

Short Title: PilU is a PilT-dependent type IVa pilus retraction ATPase

Abstract

Bacterial type IV pili are critical for diverse biological processes including horizontal gene transfer, surface sensing, biofilm formation, adherence, motility, and virulence. These dynamic appendages extend and retract from the cell surface. In type IVa pilus systems, extension occurs through the action of an extension ATPase, PilB, while optimal retraction requires the action of a retraction ATPase, PilT. Many type IVa systems also encode a homolog of PilT called PilU. However, the function of this protein has remained unclear because *pilU* mutants largely lack obvious phenotypes. Here, we study the type IVa competence pilus of *Vibrio cholerae* as a model system to define the role of PilU. We show that the ATPase activity of PilU is critical for optimal pilus retraction in PilT ATPase mutants. PilU does not, however, contribute to pilus retraction in Δ*pilT* strains. Thus, these data suggest that PilU is a *bona fide* retraction ATPase that supports pilus retraction in a PilT-dependent manner. We also found that a Δ*pilU* mutant exhibited a reduction in the force of retraction suggesting that PilU is important for generating maximal retraction forces. Additional *in vitro* and *in vivo* data show that PilT and PilU act as independent homo-hexamers that likely form a complex to facilitate pilus retraction. Finally, we demonstrate that the role of PilU as a PilT-dependent retraction ATPase is conserved in *Acinetobacter baylyi*, suggesting that the role of PilU described here may be broadly applicable to diverse type IVa pilus systems.

Author Summary

Almost all bacterial species use thin surface appendages called pili to interact with their environments. These structures are critical for the virulence of many pathogens and represent one major way that bacteria share DNA with one another, which contributes to the spread of antibiotic resistance. To carry out their function, pili dynamically extend and retract from the

43 bacterial surface. Here, we show that retraction of pili in some systems is determined by the
44 combined activity of two motor ATPase proteins.

45

46 Introduction

47 Type IV pili are ubiquitous surface appendages in Gram-negative bacteria that promote diverse
48 activities including attachment, virulence, biofilm formation, horizontal gene transfer, and
49 twitching motility [1-5]. These structures can dynamically extend and retract from the cell
50 surface, which is often critical for their function. A detailed mechanistic understanding of pilus
51 dynamic activity, however, remains lacking.

52 Type IV pili are composed almost exclusively of a single protein called the major pilin, which
53 forms a helical fiber that extends from the cell surface [6]. Extension and retraction of the pilus is
54 hypothesized to occur through the interaction of cytoplasmic hexameric ATPases with the inner
55 membrane platform of the pilus machine, whereby ATP hydrolysis likely facilitates turning of the
56 platform in order to incorporate or remove major pilin subunits from the pilus fiber [7-9]. All type
57 IV pilus systems encode a predicted ATPase (PilB) that facilitates pilus extension [7, 10-12].
58 The type IVa pilus systems also contain a retraction ATPase (PilT) which depolymerizes the
59 pilus fiber and recycles pilin subunits into the inner membrane. Many type IVa pilus systems
60 also encode another putative ATPase called PilU. PilU is a homolog of the retraction ATPase
61 PilT, however, the function of this protein has remained unclear in most pilus systems because
62 *pilU* mutants largely lack obvious phenotypes. A notable exception is *Pseudomonas aeruginosa*,
63 where *pilU* mutants exhibit reduced twitching motility [13].

64 The facultative bacterial pathogen *Vibrio cholerae* uses a type IV competence pilus for DNA
65 uptake during natural transformation. We have recently demonstrated that the type IV
66 competence pili of *V. cholerae* can be fluorescently labeled by using a technique [14-16] in

67 which an amino acid of the major pilin subunit PilA is replaced with a cysteine (PilA^{S67C}) [17],
68 which allows for subsequent labeling with a fluorescently-labeled thiol-reactive maleimide dye
69 (AF488-mal). This labeling approach does not impede dynamic pilus activity and allows for the
70 direct observation and measurement of pilus extension and retraction by time-lapse
71 epifluorescence microscopy. Using this labeling technique, we have recently demonstrated that
72 the retraction of DNA-bound type IV competence pili is required to initiate the process of DNA
73 uptake during natural transformation [17].

74 Here, we employ our pilus labeling approach and complementary molecular methods to address
75 the role that PilU plays in type IV competence pilus retraction, and we extend our findings to the
76 type IVa competence pilus of *Acinetobacter baylyi*. Our results indicate that PilT and PilU form
77 independent homo-hexamers and that the ATPase activity of PilU promotes type IV pilus
78 retraction in a PilT-dependent manner.

79

80 Results

81

82 PilU promotes type IV competence pilus retraction in a PilT-dependent manner

83 In order to study the function and role of ATPases in the retraction of type IV competence pili in
84 *V. cholerae*, we utilize two main methods: (1) our labeling approach to directly measure pilus
85 retraction via epifluorescence time-lapse microscopy and (2) assessing natural transformation,
86 which is dependent on competence pilus retraction [17, 18]. Also, as for other pili [19-21],
87 competence pili can mediate cell-to-cell interactions, which causes hyperpiliated strains to
88 aggregate and pellet to the bottom of culture tubes [22]. Consistent with prior work [17, 18, 23-
89 28], mutant strains that lack the retraction ATPase PilT are poorly transformable, exhibit
90 markedly reduced rates of pilus retraction, aggregate, and are hyperpiliated (≥3 pili per cell)

91 compared to the parent strain (**Fig 1A-D**). Qualitatively, the number of cells that exhibit dynamic
92 pilus activity is reduced in the Δ*pilT* strain as observed by time-lapse epifluorescence
93 microscopy, which is consistent with the hyperpiliated phenotype of this mutant. The residual
94 retraction in a Δ*pilT* strain is not due to PilU because a Δ*pilT* Δ*pilU* double mutant strain displays
95 the same phenotype as a Δ*pilT* strain (**Fig 1A-D**). By contrast, Δ*pilU* mutants are largely
96 indistinguishable from the parent, other than a ~1.3-fold reduction in the rate of pilus retraction
97 (**Fig 1B**). Thus, these data support a model where PilT plays the dominant role in pilus
98 retraction, which is consistent with prior reports [17, 18, 26].

99 PilT is a predicted ATPase and its ATPase activity has been shown to be important in the
100 function of other type IV pilus systems [12, 29]. Therefore, we hypothesized that the ATPase
101 activity of PilT would be required for retraction of the competence pilus. We found, however, that
102 strains harboring mutations in PilT that ablate the ATPase activity of this protein—due to a
103 mutation in either an invariantly conserved lysine in the Walker A motif required for ATP binding
104 ($pilT^{K136A}$), a mutation in a conserved glutamic acid in the Walker B motif required for ATP
105 hydrolysis ($pilT^{E204A}$), or a double mutant containing both mutations ($pilT^{E204A/K136A}$)— all
106 transform similarly to the parent strain and retract competence pili at rates that are at most ~4-
107 fold lower than the parent (**Fig 1A-B**). This is in stark contrast to a Δ*pilT* strain where the
108 transformation frequency is reduced ~4-logs and retraction is >50-fold slower compared to the
109 parent strain (**Fig 1A-B**). These results were quite surprising and suggested that either (1) the
110 ATPase activity of the retraction machinery is not critical for promoting optimal pilus retraction or
111 (2) that another retraction ATPase may promote retraction in the absence of PilT ATPase
112 activity.

113 We tested the latter model and specifically assessed whether PilU could promote retraction in
114 PilT ATPase-deficient mutants. Indeed, we found that $pilT^{K136A}$Δ*pilU*, $pilT^{E204A}$Δ*pilU* and
115 $pilT^{E204A/K136A}$Δ*pilU* strains all display reduced transformation, are hyperpiliated, aggregate, and

116 exhibit markedly reduced retraction rates similar to a Δ*pilT* Δ*pilU* strain (**Fig 1A-D**). This is
117 consistent with PilU promoting retraction in the *pilT*^{K136A}, *pilT*^{E204A} and *pilT*$^{E204A/K136A}$
118 backgrounds. Importantly, the *pilT*^{K136A}Δ*pilU*, *pilT*^{E204A}Δ*pilU* and *pilT*$^{E204A/K136A}$Δ*pilU* strains could
119 be complemented via ectopic expression of *pilT* or *pilU* (**S1 Fig**). Since loss of *pilT* alone (i.e.
120 Δ*pilT*) results in a phenotype comparable to a Δ*pilT* Δ*pilU* mutant, this result indicates that PilU
121 is not sufficient to drive pilus retraction in the absence of PilT (**Fig 1A-D**). Consistent with this,
122 ectopic expression of *pilU* does not rescue the transformation deficit of a Δ*pilT* Δ*pilU* mutant (**S1**
123 **Fig**). Together, these data suggest that PilU supports pilus retraction in a PilT-dependent
124 manner.

125 Interestingly, the *pilT*^{E204A} strain is hyperpiliated (**Fig 1D**). Qualitatively, the frequency of cells
126 that exhibit pilus retraction in this mutant is much lower than the parent and comparable to the
127 Δ*pilT* Δ*pilU* strain (as assessed by epifluorescence time-lapse microscopy), which may explain
128 this hyperpiliated phenotype; however, when pilus retraction is observed, the rate of retraction is
129 closer to that of the parent than the Δ*pilT* Δ*pilU* mutant (**Fig 1B**). Considering the canonical
130 functions of the Walker A and B motifs in ATP-binding and hydrolysis, respectively, the Walker
131 B *pilT*^{E204A} mutant should be able to bind to ATP but not hydrolyze it. Because the ATP-binding
132 deficient *pilT*^{K136A} Walker A mutant exhibited parental levels of piliation (**Fig 1D**), we
133 hypothesized that the hyperpiliation observed in *pilT*^{E204A} may be due to the ATP-binding state
134 of this mutant. Consistent with this, we found that the Walker A and B double mutant
135 (*pilT*$^{E204A/K136A}$) exhibits parent levels of piliation in contrast to the *pilT*^{E204A} single mutant (**Fig**
136 **1D**). These results indicate that the phenotype of the ATP-binding deficient Walker A mutant
137 (*pilT*^{K136A}) is dominant over the ATP-hydrolysis deficient *pilT*^{E204A} Walker B mutation. Both of
138 these mutations should result in loss of ATPase activity. Therefore, to avoid phenotypic
139 consequences of variable states of ATP binding associated with the *pilT*^{E204A} mutant, we utilized
140 the *pilT*^{K136A} mutant as an ATPase-defective allele of PilT moving forward.

141

142 **PilU is required for forceful retraction**

143 The data thus far suggest that PilU is sufficient but not necessary to mediate pilus retraction and
144 natural transformation. However, PilU is present in many type IVa pilus systems, so the
145 question remains: Why is PilU so widely conserved if it is not necessary for pilus retraction?
146 Recent work in *Pseudomonas aeruginosa* indicates that PilU may be required for forceful
147 retraction [30]. Our data thus far indicate that pilus retraction in the *pilU* mutant is largely
148 indistinguishable from the parent (**Fig 1B**), however, these measurements are based on free pili
149 that are not retracting under load. We hypothesized that PilU might be required for forceful
150 retraction, such as when pili are attached to a surface. To test this, we assessed pilus retraction
151 using a micropillar assay in which binding of pili to micropillars and subsequent retraction results
152 in measurable bending and displacement of the micropillars. These data can then be used to
153 calculate the rates and force of pilus retraction [31]. In this assay, the Δ*pilU* mutant exhibited a
154 significant reduction in retraction force (~2-fold) and speed (~3-fold) compared to the parent
155 strain, despite the fact that this strain still has functional PilT-dependent retraction (**Fig 1B,E-F**).
156 This reduction in the force of retraction in the Δ*pilU* mutant is comparable to the reduction in
157 force of retraction observed in the Δ*pilT* mutant (**Fig 1E**). Thus, these data indicate that PilU is
158 necessary for generating maximal retraction forces in the *V. cholerae* competence pilus.

159

160 **The ATPase activities of PilT and PilU define the rate of type IV competence pilus**
161 **retraction**

162 Just like PilT, PilU is a AAA family ATPase with a conserved lysine in its Walker A motif.
163 Because we observed that PilU supports pilus retraction in the $pilT^{K136A}$ mutant (**Fig 1B**), we
164 hypothesized that the ATPase activity of PilU may be important for supporting pilus retraction.

165 To test the relative roles of each of these ATPases in pilus retraction, we mutated the conserved
166 lysine in the Walker A motifs of PilT and/or PilU. The *pilU*^{K134A} strain retracts ~1.5-fold slower
167 than the parent strain, similar to the Δ*pilU* mutant (**Fig 2A**). There may be a limited effect of the
168 *pilU*^{K134A} mutation on pilus retraction because this strain still has a functional PilT ATPase.
169 However, we hypothesized that PilU ATPase activity may be critical for retraction in a
170 background where PilT ATPase activity is also inactivated. Consistent with this, we found that a
171 *pilT*^{K136A} *pilU*^{K134A} strain is indistinguishable from a Δ*pilT* strain for pilus retraction, piliation,
172 aggregation, and transformation (**Fig 2A-C**). Together, these data suggest that PilU ATPase
173 activity promotes type IV competence pilus retraction.

174 The data above suggest that the ATPase activities of PilT and PilU are critical for pilus
175 retraction. These ATPases are predicted to be motor proteins that facilitate the depolymerization
176 of pilus fibers. Thus, if we alter the ATPase rates of these motors, we hypothesized that this
177 should alter the rates of pilus retraction. To test this hypothesis, we mutated a leucine in the
178 Walker B domain of PilT and PilU to a cysteine, which was previously shown to reduce the rate
179 of ATP hydrolysis of *Neisseria gonorrhoeae* PilT ~2-fold [26]. When these Walker B mutations
180 were tested in isolation they did not alter the rate of pilus retraction (Comparing Parent strain to
181 *pilT*^{L201C} and *pilU*^{L199C}) (**Fig 2A**). This may be due to the fact that these cells still have one fully
182 functional retraction ATPase (i.e. *pilT*^{L201C} still has a fully functional PilU and *pilU*^{L199C} still has a
183 fully functional PilT). We hypothesized that these Walker B "slow" ATPase mutations, however,
184 may have an impact on pilus retraction if they represented the sole functional retraction ATPase
185 in the cell. To that end, we generated both a *pilT*^{L201C} Δ*pilU* strain and a *pilT*^{K136A} *pilU*^{L199C} strain.
186 In both cases, these strains exhibited reduced retraction rates relative to the appropriate parent
187 strain: a ~1.3-fold reduction for PilT^{L201C} (comparing *pilT*^{L201C}Δ*pilU* to Δ*pilU*) and an ~1.5-fold
188 reduction for PilU^{L199C} (comparing *pilT*^{K136A}*pilU*^{L199C} to *pilT*^{K136A}) (**Fig 2A**). This provides genetic
189 evidence that the ATPase activities of PilT and PilU are linked to the retraction rate of the type

190 IV competence pilus. Furthermore, it provides additional supporting evidence that PilU promotes
191 pilus retraction through its ATPase activity.

192

193 **PilT and PilU directly interact with one another**

194 All of the data presented above indicate that PilT and PilU can both support pilus retraction.
195 Therefore, we hypothesized that PilT and PilU may interact to form a complex that supports
196 pilus retraction. To address this, we utilized a Bacterial Adenylate Cyclase Two-Hybrid (BACTH)
197 assay [32, 33]. As expected for predicted hexameric proteins like PilT and PilU, the BACTH
198 analysis showed PilT-PilT and PilU-PilU self-interactions (**Fig 3** and **S2 Fig**). Additionally, the
199 BACTH assay showed that PilT and PilU interact with one another and that the Walker A
200 mutations of either protein ($PilT^{K136A}$ and $PilU^{K134A}$) did not disrupt this interaction (**Fig 3** and **S2**
201 **Fig**). Thus, our BACTH results suggest that PilT and PilU may form a complex to mediate pilus
202 retraction. These results do not, however, indicate whether PilU and PilT form heteromeric
203 complexes or homomeric complexes to facilitate pilus retraction. We test this further below.

204

205 **PilT and PilU form independent homohexameric rings in vitro and in vivo**

206 PilT in other systems has been shown to form a hexameric complex [34], and by homology we
207 hypothesized that PilU also forms a hexamer. Based on transformation frequency assays, N-
208 terminally tagged ^{6X}His-PilT and ^{6X}His-PilU were fully functional (**S3A Fig**). Therefore, we
209 purified ^{6X}His-PilT and ^{6X}His-PilU to characterize these proteins *in vitro*. Negative stain
210 transmission electron microscopy revealed that both ^{6X}His-PilT and ^{6X}His-PilU formed hexameric
211 ring complexes (**Fig 4A**). These results indicate that these proteins are capable of forming
212 independent homohexameric complexes *in vitro*. PilT and PilU have both sequence (~65%

213 similarity) and structural similarity to one another (**Fig 4A**), thus it is also possible that these
214 proteins can be incorporated into one ring and form heterohexameric complexes that facilitate
215 pilus retraction *in vivo*.

216 In order to test if PilT and PilU form heterohexamers or independent homohexamers to facilitate
217 pilus retraction *in vivo*, we hypothesized that overexpression of ATPase-inactive mutants (i.e.
218 PilT^{K136A} and PilU^{K134A}) in backgrounds that have native PilT and PilU would allow us to
219 distinguish between these two models. For example, if these proteins form heteromeric
220 complexes, then we would predict that overexpression of either ATPase-inactive protein
221 (PilT^{K136A} or PilU^{K134A}) should result in complexes that are mostly composed of ATPase-inactive
222 proteins and result in inhibition of pilus retraction (yielding a hyperpiliated phenotype) and
223 reduce rates of natural transformation (**Fig 4B**). If these proteins solely form homomeric
224 complexes, however, then we would predict that overexpression of only one ATPase-inactive
225 protein (PilT^{K136A} or PilU^{K134A}) should only inhibit the activity of one motor complex (PilT or PilU,
226 respectively) and should not have a dramatic effect on pilus retraction or natural transformation
227 because the other retraction motor would still be intact (**Fig 4B**).

228 In order for us to successfully test this question, we needed to: (1) be able to ectopically
229 overexpress ATPase deficient alleles of PilT or PilU, (2) demonstrate that ATPase deficient
230 alleles can interact with their ATPase sufficient counterparts and form proper hexamers, and (3)
231 show that ectopic expression of ATPase deficient alleles of PilT or PilU can inhibit the activity of
232 their respective natively expressed ATPase. We test each of these in turn below. First, we
233 confirmed that we could ectopically overexpress PilT and PilU. Using functional 3xFLAG-tagged
234 versions of PilT and PilU (**S3A-B Fig**), we show that our chromosomal P_{tac} regulated constructs
235 resulted in dramatic overexpression of these proteins (**S3C Fig**). Importantly, overexpression of
236 WT PilT and PilU did not affect pilus activity or natural transformation (**S1 and S3B,D Figs**).
237 Next, we purified ^{6X}His-PilT^{K136A} and ^{6X}His-PilU^{K134A} and demonstrated that they formed ring

238 structures *in vitro* (**S3E Fig**), indicating that these proteins should form complexes with ATPase
239 sufficient alleles. This is also supported by our BACTH data (**Fig 3**). Finally, we wanted to
240 confirm that overexpressing the ATPase-inactive PilT^{K136A} or PilU^{K134A} could effectively impede
241 the function of the natively expressed ATPase-active PilT or PilU. To test this, we genetically
242 isolated either PilT or PilU as the sole functional retraction ATPase (i.e. PilT activity is isolated in
243 a Δ*pilU* background, while PilU activity is isolated in a *pilT*^{K136A} background) and then
244 overexpressed the cognate ATPase-inactive allele (P_{tac}-*pilT*^{K136A} or P_{tac}-*pilU*^{K134A}, respectively).
245 We assessed piliation, aggregation, and natural transformation as indicators of optimal pilus
246 retraction. We found that, as expected, overexpression of ATPase-inactive alleles was sufficient
247 to disrupt the activity of the natively expressed ATPase (**Fig 4C-D** - compare Δ*pilU* to Δ*pilU* P_{tac}-
248 *pilT*^{K136A} and *pilT*^{K136A} to *pilT*^{K136A} P_{tac}-*pilU*^{K134A}). Also, as expected, overexpression of both
249 ATPase-deficient alleles together (P_{tac}-*pilT*^{K136A} and P_{tac}-*pilU*^{K134A}) in a background that has
250 natively expressed PilT and PilU, results in hyperpiliation, aggregation and reduced natural
251 transformation (**Fig 4C-D**), which further demonstrates that overexpression of these ATPase-
252 deficient proteins inhibits the activity of their natively expressed ATPase–sufficient versions.

253 The experiments above indicated that it would be feasible to test whether PilT and PilU formed
254 homomeric or heteromeric complexes *in vivo* as described in our model (**Fig 4B**). When we
255 overexpressed only one ATPase-deficient protein (P_{tac}-*pilT*^{K136A} or P_{tac}-*pilU*^{K134A}) in a background
256 that has natively expressed PilT and PilU, we found that piliation and transformation were
257 indistinguishable from the parent (**Fig. 4C-D**). Thus, these data are consistent with PilT and PilU
258 forming independent homohexamers to facilitate pilus retraction.

259 Using our purified PilT and PilU, we also attempted to directly measure the ATPase activity of
260 these proteins. Unfortunately, the ATPase activity of these purified proteins was
261 indistinguishable from contaminating ATPases and/or below our detection limit (~1 nmol
262 pi/min/mg protein). Poor ATPase activity in purified retraction ATPases is not unique to our

263 system [12, 29, 35]. This may be due to the fact that the ATPase activities of these proteins are
264 stimulated *in vivo* via interaction with the proteins that compose the pilus machine, as previously
265 suggested [12]. Regardless, our previous *in vivo* data (**Fig 1A-D**) are consistent with the
266 *pilT*^{K136A} mutant being ATPase deficient.

267

268 The presence of PilT is not required for PilU to interact with the pilus platform 269 PilC.

270 Our data thus far indicate that PilU requires the presence of PilT (whether it is a functional
271 ATPase or not) to support optimal pilus retraction. The extension and retraction ATPases are
272 hypothesized to interact with the platform protein PilC to mechanically facilitate polymerization
273 and depolymerization of the pilus fiber [7, 36, 37]. Because PilU is dependent on the presence
274 of PilT to mediate optimal retraction, we hypothesized that PilT can interact with PilC, but that
275 PilU cannot. To test this, we utilized the BACTH assay to test the interactions of PilT and PilU
276 with PilC. This assay showed that PilT and PilU could both interact with PilC, and that the
277 Walker A mutations of these ATPases (PilT^{K136A} and PilU^{K134A}) did not affect these interactions
278 (**Fig 3**). The interaction between PilC and PilT supports the canonical model that retraction
279 ATPases interact with PilC to facilitate depolymerization of the pilus fiber. Interestingly, PilC and
280 PilU interact independently of PilT. Thus, the simple model of PilU requiring PilT for interaction
281 with the platform PilC appears to be incorrect.

282

283 The function of PilU as a PilT-dependent retraction ATPase is conserved

284 As mentioned earlier, many type IVa pilus systems encode PilU in addition to the canonical
285 retraction ATPase PilT. Therefore, we sought to assess whether PilU could facilitate PilT-

286 dependent retraction in other type IV pilus systems. To test this, we studied the type IVa
287 competence pili of *Acinetobacter baylyi*.

288 The competence pili of *A. baylyi* likely facilitate DNA uptake in a retraction-dependent manner,
289 similar to the competence pili of *V. cholerae*. Thus, we employed natural transformation assays
290 to dissect the role that PilT and PilU play in *A. baylyi* competence pilus retraction. These assays
291 showed that the PilT and PilU of *A. baylyi* behave largely like the PilT and PilU of *V. cholerae*.
292 The *pilU* mutant of *A. baylyi* displays a significant (~13-fold) reduction in natural transformation
293 (**Fig 5**), unlike what is observed in *V. cholerae* (**Fig 1A**). This may be because DNA uptake in *A.*
294 *baylyi* requires more forceful retraction or because PilU plays a more important role in pilus
295 retraction in this species. Most importantly, however, we found that PilU facilitates natural
296 transformation (and therefore pilus retraction) in backgrounds where the ATPase activity of PilT
297 is inactivated, but not in backgrounds where *pilT* is absent (**Fig 5** – compare $pilT^{K136A}$ to $pilT^{K136A}$
298 Δ*pilU* and Δ*pilT*). Also, a strain where the ATPase activity of both PilT and PilU were inactivated
299 ($pilT^{K136A}$ $pilU^{K137A}$) resulted in the loss of transformation equivalent to a retraction deficient
300 background (e.g. Δ*pilTU*) or a strain lacking competence pili (Δ*comP*). Importantly, strains
301 lacking *pilT* (i.e. Δ*pilT* and Δ*pilTU*) could only be complemented via ectopic expression of *pilT*
302 but not *pilU*, while strains that contained an ATPase defective allele of *pilT* (i.e. $pilT^{K136A}$ Δ*pilU* or
303 $pilT^{K136A}$ $pilU^{K137A}$) could be complemented by ectopic expression of *pilT* or *pilU* (**S4 Fig**) These
304 data are consistent with what was observed for *V. cholerae* competence pili (**Fig 1A and S1**
305 **Fig**) and suggest that PilU ATPase activity facilitates pilus retraction in a PilT-dependent
306 manner in diverse type IVa pilus systems.

307

308 ## Discussion

309 This study sheds light on the function of PilU as a retraction ATPase of type IVa competence pili
310 in *V. cholerae*. Specifically, our data indicate that PilU can mediate pilus retraction in a PilT-
311 dependent manner likely through its ATPase activity. Our results also show that PilT and PilU
312 form independent homohexamers that likely interact to form a complex that supports pilus
313 retraction. Furthermore, we demonstrate that the role of PilU in supporting pilus retraction is
314 conserved in at least one other type IVa pilus system.

315 Our results indicate that PilU can only facilitate pilus retraction in the presence of PilT,
316 regardless of whether that PilT is a functional ATPase. These results are also supported by a
317 recent preprint from the Blokesch lab [22]. We initially tested the hypothesis that this was due to
318 a requirement for PilT to bridge PilU with the platform protein PilC. Our BACTH results,
319 however, indicated that PilU may directly interact with PilC in the absence of PilT. While they
320 may interact, it is possible that PilU does not bind and engage the PilC platform in a
321 conformation that would facilitate retraction. Alternatively, it is possible that PilU does bind PilC
322 in a conformation that can facilitate retraction but additional interactions with PilT are required to
323 stimulate PilU ATPase activity. Another possibility is that PilT interacts with other components of
324 the pilus machine that are required for stimulating retraction, and that PilU lacks these
325 interactions. Future efforts focused on the interaction network of the retraction ATPases with the
326 pilus machine should shed light on this question.

327 Previous reports have shown that PilU is necessary for twitching motility in *P. aeruginosa* [13],
328 an activity that likely requires forceful retraction [30]. Consistent with this, our results indicate
329 that PilU is necessary for maximal retraction force for the competence pilus in *V. cholerae*.
330 Interestingly, because the Δ*pilU* mutant transforms similarly to the parent strain (**Fig 1B** and
331 **2A**), the forceful retraction mediated by PilU does not seem to be necessary for the function of
332 the *V. cholerae* competence pilus in DNA uptake under the conditions tested. However, forceful

333 PilU-dependent retraction may be necessary for DNA uptake when tDNA is absorbed onto
334 surfaces and/or in complex environments like biofilms.

335 Beyond altering the force of retraction, many mutants in PilT and PilU also reduced the speed of
336 pilus retraction (i.e. Δ*pilU* = ~1.3-fold, $pilT^{K136A}$ = ~4.3-fold, $pilT^{K136A}$ $pilU^{L199C}$ = ~6.5-fold, $pilU^{K134A}$
337 = ~1.5-fold, $pilT^{L201C}$ Δ*pilU* = ~1.7-fold). This revealed that altering the rates of these motor
338 ATPases results in a corresponding reduction in the rate of pilus retraction. Additionally, despite
339 this reduction in the speed of pilus retraction, these mutants still transformed at levels that were
340 comparable to the parent strain. Thus, these results suggest that the absolute speed of
341 competence pilus retraction is not critical for DNA uptake during natural transformation. Further
342 experiments will focus on defining the parameters that are essential for DNA uptake.

343 Mutants that completely inactivated the retraction machinery (e.g. Δ*pilT*, Δ*pilT* Δ*pilU*, $pilT^{K136A}$
344 Δ*pilU*, $pilT^{K136A}$ $pilU^{K134A}$) resulted in a hyperpiliated phenotype, lower transformation frequency
345 and a marked reduction in the frequency of pilus retraction (as observed qualitatively by
346 epifluorescence time-lapse microscopy). These strains, however, did display rare pilus
347 retraction, which occurred at rates that were markedly slower than the parent (>40-fold), which
348 is independent of PilT and PilU. Recent work in *Neisseria* indicates that PilTU-independent
349 retraction is not unique to the *V. cholerae* competence pilus [38]. The mechanism underlying
350 PilTU-independent retraction is still unclear [5] and will be the focus of future work.

351

352 ## Materials and Methods

353

354 ### Bacterial strains and culture conditions

355 *Vibrio cholerae* and *A. baylyi* strains were routinely grown in LB Miller broth and on LB Miller
356 agar supplemented with erythromycin (10 µg/mL), kanamycin (50 µg/mL), and/or carbenicillin
357 (50 µg/mL) when appropriate.

358

359 **Construction of mutant strains**

360 All *V. cholerae* strains used throughout this study are derivatives of the El Tor isolate E7946. All
361 *A. baylyi* strains used were derivatives of strain ADP1 [39]. All mutant strains were constructed
362 via MuGENT and natural transformation using transforming DNA products made by splicing-by-
363 overlap extension (SOE) PCR exactly as previously described [40-43]. For a detailed list of all
364 mutant strains used throughout this study see **Table S1**. For a detailed list of all primers used to
365 construct mutant strains see **Table S2**.

366

367 **Natural transformation assays**

368 In order to induce competence in *V. cholerae* strains, the master competence regulator TfoX
369 was overexpressed using an IPTG-inducible or constitutive P_{tac} promoter and the cells were
370 genetically locked in a state of high cell density via deletion of *luxO* [41, 44-48]. Chitin-
371 independent transformation assays were performed exactly as previously described [42]. Briefly,
372 strains were grown overnight rolling at 30 ^{o}C with 100 µM IPTG then ~10^8 colony forming units
373 (CFU) were subcultured into 3mL of LB + 100 µM IPTG + 20 mM $MgCl_2$ + 10 mM $CaCl_2$ and
374 grown to late log. Next, ~10^8 CFU of this culture was diluted into instant ocean medium (7 g/L;
375 Aquarium Systems) supplemented with 100 µM IPTG and 500ng of transforming DNA was
376 added to each reaction and incubated statically at 30 ^{o}C overnight. The tDNA targeted VC1807,
377 a frame-shifted transposase, for deletion as previously described [40]. Negative control
378 reactions where no tDNA was added were also performed for each strain. After incubation with

379 tDNA, reactions were outgrown by adding 1mL of LB to each reaction and shaking (250 rpm) at
380 37 ^{o}C for ~2 hours. Reactions were then plated for quantitative culture onto medium selecting for
381 transformants (LB + 10 µg/mL Erythromycin) or onto plain LB for total viable counts. The
382 transformation frequency is defined as the number of transformants divided by the total viable
383 counts. For reactions where no transformants were obtained, a limit of detection was calculated
384 and plotted.

385 In order to sensitize natural transformation assays to differences in the efficiency of DNA
386 uptake, reactions were incubated with transforming DNA for shorter periods of time. These
387 assays were prepared exactly as described above, except that 10 units of DNase I (NEB) was
388 added to reactions 7 minutes after incubation with 500ng of transforming DNA. Reactions were
389 then incubated statically at 30°C overnight, outgrown, and plated exactly as described above.

390 For *A. baylyi*, transformations were performed exactly as previously described [49]. Briefly,
391 strains were grown overnight in LB medium. Then, ~10^8 cells were diluted into fresh LB
392 medium, and tDNA was added (~100 ng). Reactions were incubated at 30°C with agitation for 5
393 h and then plated for quantitative culture as described above to determine the transformation
394 frequency.

395

396 **Pilin labelling, imaging and quantification**

397 In order to label pili for observation with epifluorescence microscopy, strains were grown to the
398 late-log phase exactly as described above for natural transformation assays. Then, ~10^8 CFU
399 were spun down at 18,000 x g for 1 min and resuspended in instant ocean medium. Cells were
400 then incubated with 25 µg/mL AF488-mal for 15 minutes statically at room temperature in the
401 dark. Cells were washed twice using 100µL of instant ocean medium and resuspended to a final
402 concentration of ~10^7 CFU. Next, 2µL of these labeled cells were placed under an 0.2% gelzan

403 pad (made in instant ocean medium) on a coverslip and imaged on an inverted Nikon Ti-2
404 microscope with a Plan Apo ×60 objective, a green fluorescent protein filter cube, a Hamamatsu
405 ORCAFlash 4.0 camera and Nikon NIS Elements imaging software. In order to measure
406 retraction events, labelled cells were imaged by time-lapse microscopy in which a phase-
407 contrast (to image cell bodies) and fluorescent (to image labeled pili) image were taken every
408 second for 1-2 minutes or every 10 seconds for 10-15 minutes. Rates were calculated manually
409 using measurement tools in the NIS Elements analysis software. Only pili that were longer than
410 0.3 µm and completed retracting within the time-lapse window were analyzed.

411 In order to calculate the number of pili per cell, static images of cell bodies and labeled pili were
412 captured using phase-contrast and epifluorescence microscopy, respectively. Images from 3
413 independent biological replicates were sectioned into areas containing ~100-200 cells and the
414 total number of cells and the number of pili displayed on each cell was manually determined.
415 Representative images of the piliation state of strains were gathered and the lookup tables for
416 each phase or fluorescent image were adjusted to the same range.

417 To assess aggregation and pelleting of cultures, strains were grown to late log under the
418 conditions described above. Cultures were then allowed to sit statically at room temperature for
419 30-60 mins. Images of cultures were then taken against a white background.

420

421 **Protein expression and purification**

422 His tagged (6xHis) versions of PilT, PilT^{K136A}, PilU and PilU^{K134A} were cloned into a pHis
423 expression vector and verified by DNA sequencing (Eurofins). Vectors were transformed into *E.*
424 *coli* BL21 DE3 for expression and purification.

425 For purification of His-PilU and His-PilU^{K134A}, cells were grown in a 1L flask at 37°C with aeration
426 to an OD_{600} = 0.6. The culture was then induced by adding IPTG (1 mM) and grown to a final

427 OD_{600} = 4.0 at 30°C with aeration. Cells were harvested by centrifugation at 8,000 x g for 15 min
428 at room temperature and then resuspended in Buffer A [100 mM Tris pH 8.5, 300 mM KCl, 10%
429 glycerol, 20 mM Imidazole] and stored at -80°C. Pellets were thawed on ice and then lysozyme
430 (1 mg/mL) and DNase I (2 mg/L) were added before lysing via sonication with a probe tip
431 sonicator. The soluble fraction was clarified by centrifugation at 12,000 x g for 1 hour at 4°C.
432 The supernatant was loaded onto a nickel-charged HisTrap HP column (1mL; GE) using an
433 ÄKTA FPLC at room temperature. The column was then washed with Buffer A and the protein
434 was eluted with a gradient of Buffer B [100 mM Tris pH 8.5, 300 mM KCl, 10% glycerol, 500 mM
435 imidazole] and fractions were collected on ice. Elution fractions were separated on 15% SDS-
436 PAGE gels and stained with Coomassie Brilliant Blue R-250 (BioRad). Peak fractions were
437 pooled and dialyzed (Fisher, MWCO 12 kDa) into 500 mL Buffer C [100 mM Tris pH 8.5, 300
438 mM KCl, 10% glycerol] overnight, on a stir plate at 4°C. Then a second round of dialysis was
439 performed using 500 mL Buffer C for 4-6 hours, on a stir plate at 4°C. Following dialysis, the
440 protein concentration was determined using a Bradford Assay and aliquots were stored at -80C.

441 For purification of His-PilT and His-PilT^{K136A}, cells were grown in a 1L flask at 37°C with aeration
442 to an OD_{600} = 0.6. The culture was then induced by adding IPTG (1 mM) and grown overnight at
443 22°C with aeration. Cells were harvested by centrifugation at 8,000 x g for 15min at room
444 temperature and then resuspended in Buffer A [25 mM Tris pH 8.5, 300 mM KCl, 10% glycerol,
445 1 mM EDTA, 1 mM $MgCl_2$, 5 mM β-mercaptoethanol, 20 mM Imidazole] and stored at -80°C.
446 Pellets were thawed on ice and lysozyme (1 mg/mL), DNase I (2 mg/L) and PMSF (1 mM) were
447 added before lysing via sonication with a probe tip sonicator. The soluble fraction was clarified
448 by centrifugation at 12,000 x g for 1 hour at 4°C. The supernatant was loaded onto a nickel-
449 charged HisTrap HP column (1 mL; GE) using an ÄKTA FPLC at room temperature. The
450 column was then washed with Buffer A and the protein was eluted with a gradient of Buffer B
451 [25 mM Tris pH 8.5, 300 mM KCl, 10% glycerol, 1 mM EDTA, 1 mM $MgCl_2$, 5 mM β-

452 mercaptoethanol, 500 mM Imidazole] and fractions were collected on ice. Elution fractions were
453 separated on 15% SDS-PAGE gels and stained with Coomassie Brilliant Blue R-250 (BioRad).
454 Peak fractions were pooled and dialyzed (Fisher, MWCO 12 kDa) into 500 mL Buffer C [25 mM
455 Tris pH 8.5, 50 mM KCl, 10% glycerol, 1 mM EDTA, 1 mM $MgCl_2$, 0.5mM TCEP] overnight, on a
456 stir plate at 4°C. The next day, the eluate was concentrated with an Amicon conical filter
457 (MWCO 30 kDa) at 4,000 x g for 15 min at 4°C and resuspended to the original volume in Buffer
458 C twice. The protein concentration was determined using a Bradford Assay and then aliquots of
459 protein were snap-frozen with liquid nitrogen and stored at -80C.

460

461 **Bacterial Adenylate Cyclase Two-hybrid (BACTH) Assays**

462 The Bacterial Adenylate Cyclase Two-Hybrid (BACTH) system was employed to study protein
463 interactions. Gene inserts were amplified by PCR and cloned into pUT18C ($Carb^R$) and pKT25
464 (Kan^R) vectors to generate N-terminal fusions to the T18 and T25 fragments of adenylate
465 cyclase, respectively. Miniprepped vectors (Qiagen plasmid miniprep kit) were then
466 cotransformed into *E. coli* BTH101 and outgrown with 500 µL LB for 1 hour at 37°C with
467 shaking. Transformations were isolation streak plated on LB plates containing kanamycin 50
468 µg/mL and carbenicillin 100 µg/mL to select for transformants that had received both plasmids.
469 Strains were then grown statically at 30°C from frozen stocks overnight in LB supplemented with
470 kanamycin 50 µg/mL and carbenicillin 100 µg/mL and 3.5µL of each strain was then spotted
471 onto LB plates containing kanamycin 50 µg/mL, carbenicillin 100µg/mL, 0.5 mM IPTG and 40
472 µg/mL X-gal and incubated at 30°C for 48 hours.

473

474 **BACTH Miller Assays**

475 For BACTH Miller assays strains were prepared by growing the BTH101 strains with the
476 indicated pUT18C and pKT25 vectors statically overnight at 30°C in LB supplemented with
477 kanamycin 50 µg/mL and carbenicillin 100 µg/mL. Then 5 µL of this overnight culture was
478 subcultured into 3mL of LB supplemented with kanamycin 50 µg/mL, carbenicillin 100µg/mL and
479 0.5 mM IPTG and grown rolling at 30°C overnight. Cultures were then pelleted and resuspended
480 in 1 mL of Z buffer [60 mM Na_2HPO_4-$7H_2O$, 40 mM NaH_2PO_4-H_2O, 10 mM KCl, 2 mM $MgSO_4$-
481 $7H_2O$] to an OD_{600} = 0.5. 50µL of 1% SDS was added to each reaction and vortexed. 100µL of
482 chloroform was added to each reaction, vortexed again and then centrifuged for 1 min at 18,000
483 x g. The aqueous fraction was then mixed with ONPG (2.5 mg/mL) in a 96-well plate and the
484 OD_{420} and OD_{550} were measured every 5 minutes for 10 hours. Miller units were then calculated
485 at the time (in mins) when the A_{420} reached 0.3 or at 10 hours using the formula: [1000*(A_{420}-
486 (1.75*A_{550}))/ (mins*0.2 mL*A_{600})].

487

488 **Western Blotting**

489 Strains were grown to mid-log phase in LB with 100 µM IPTG if applicable and then
490 resuspended to an OD_{600} = 100 in TBS containing 1 mM PMSF. Cells were then lysed using a
491 FastPrep-24 (MP Bio). Lysates were centrifuged at 16,000 x g for 10 min at 4°C, and the
492 supernatant was then mixed 1:1 with 2X SDS sample buffer [220 mM Tris pH 6.8, 25% glycerol,
493 1.8% SDS, 0.02% Bromophenol Blue, 5% β-mercaptoethanol] and then 2uL of each sample
494 was separated on a 15% SDS PAGE gel. Proteins were transferred to a PVDF membrane and
495 incubated with one of the following primary antibodies: α-FLAG polyclonal rabbit (Sigma) or α-
496 RpoA monoclonal mouse (Biolegend). Then, blots were washed and incubated with a α-rabbit
497 or α-mouse secondary antibodies conjugated to IRdye 800CW. Blots were then imaged using
498 an Odyssey classic LI-COR system.

499

500 **Negative-stain electron microscopy**

501 Negative stain specimens were prepared by applying 4 µL of protein solution (0.1 mg/mL + 1
502 mM AMP-PnP) onto a glow-discharged 300-mesh copper grid coated with continuous carbon
503 film (EMS). After 30 s the protein solution was blotted with a piece of filter paper. The grid was
504 washed with 4 µL of milli-Q water and stained with 4 µL of stain solution (1% (w/v) uranyl
505 acetate, 0.5% (w/v) trehalose). The excess stain solution was removed by filter paper and the
506 grid was left to air dry. Due to the availability of the instrument, we used two different
507 transmission electron microscopes for data collection. For PilU, the data were collected on a
508 300-kV JEM-3200FS TEM equipped with FEG source and 8k x 8k Direct Electron DE-64
509 camera. A total of 32 micrograph images were taken at a nominal magnification of 60,000x,
510 which is equivalent to 1.56 Å per pixel. For PilT, the data were collected on a 120-kV JEM-
511 1400plus TEM equipped with LaB_6 source and a Gatan Oneview camera. A total of 59 images
512 were taken at a nominal magnification of 60,000x and the pixel size is 1.94 Å. To avoid potential
513 beam induced damage, minimum dose system was employed during data collection. Note that
514 PilU data were collected on a direct electron detector; therefore, each image contains 50 frames
515 and the frame alignment was performed using unblur program with exposure filter applied.
516 Particle picking, defocus estimation and phase flipped particles were all done using EMAN2
517 software package [50]. These particles were then imported into RELION (v2.1) for 2D
518 classification, Initial model building, 3D refinement, and 3D classification [51]. From 2D
519 classification results, we observed clearly 6-fold symmetry; thus, the symmetry operation was
520 applied to subsequent 3D refinement and 3D classification. The final 3D reconstructions were
521 computed from 45204 particles to 13.1 Å for PilU and 17472 particles to 14.7 Å for PilT. The
522 resolution estimation was calculated using gold-standard method at Fourier shell correlation of
523 0.143 as implemented in RELION. However, due to the nature of the negative stain, the
524 effective resolution could be equal to or worse than 15 Å. The 3D reconstructions were rendered

525 using UCSF Chimera where the handedness of PilU was chosen to be consistent with PilT
526 [52].
527

528 **Micropillar retraction assay**

529 To ensure that all measurements recorded were due to type IV competence pili, all the
530 experiments were performed with *V. cholerae* strains lacking all external appendages other than
531 type IV competence pili as well as exopolysaccharide production (i.e. mutants lacking flagella,
532 MSHA pili, TCP pili and *Vibrio* polysaccharide (VPS) production). Strains were grown overnight
533 in LB either directly from frozen stocks or from a single colony from an LB agar plate. Of the
534 overnight liquid culture, 50 µl was subcultured into 3 ml LB + 100 µM IPTG + 20 mM $MgCl_2$ + 10
535 mM $CaCl_2$ and allowed to grow at 30°C for 4h. Then, 100 µl of this culture was centrifuged for 5
536 min at 20,000 x *g* and the bacteria were resuspended in instant ocean medium. At different
537 times, 23 µl of the resuspension were added to micropillars in an observation chamber as
538 previously reported [15]. Briefly, silica molds were inverted on activated coverslips with
539 polyacrylamide gels in between. The result is an array of flexible micropillars in a hexagonal
540 array of 3 µm × 3 µm.Once the bacteria were in contact with the micropillars, 10-Hz movies of
541 the top of the pillars were recorded. The motion of the tips of the pillars was tracked using a
542 cross-correlation algorithm in ImageJ. The amplitude and speeds of the pillars' motions were
543 then analyzed using MATLAB. Finally, we calibrated the pillars' stiffness constant using optical
544 tweezers as previously described [31]. The pillars used in this study have a stiffness constant of
545 17±4pNµm−1.

546

547 **Statistics**

548 Statistical differences were assessed by two-tailed Student's t-tests using GraphPad Prism
549 software.

550

551 ## Acknowledgements

552 We would like to thank CK Ellison for helpful discussions. We would like to acknowledge JD
553 Newman and CE Dann III for their advice during protein purification. We thank JC van Kessel
554 for providing BACTH strains and plasmids, and Lakshay Khosla and Vijay Deopersaud for
555 technical assistance with micropillar experiments. This work was supported by grants
556 R35GM128674 and AI118863 from the National Institutes of Health to ABD, and by grant
557 AI116566 from the National Institutes of Health to NB.

558

559 ## References

560 1. Burrows LL. Pseudomonas aeruginosa twitching motility: type IV pili in action. Annu Rev
561 Microbiol. 2012;66:493-520. doi: 10.1146/annurev-micro-092611-150055. PubMed PMID:
562 22746331.
563 2. Maier B, Wong GCL. How Bacteria Use Type IV Pili Machinery on Surfaces. Trends
564 Microbiol. 2015;23(12):775-88. doi: 10.1016/j.tim.2015.09.002. PubMed PMID: 26497940.
565 3. Hospenthal MK, Costa TRD, Waksman G. A comprehensive guide to pilus biogenesis in
566 Gram-negative bacteria. Nat Rev Microbiol. 2017;15(6):365-79. Epub 2017/05/13. doi:
567 10.1038/nrmicro.2017.40. PubMed PMID: 28496159.
568 4. Proft T, Baker EN. Pili in Gram-negative and Gram-positive bacteria - structure,
569 assembly and their role in disease. Cell Mol Life Sci. 2009;66(4):613-35. Epub 2008/10/28. doi:
570 10.1007/s00018-008-8477-4. PubMed PMID: 18953686.

571 5. Craig L, Forest KT, Maier B. Type IV pili: dynamics, biophysics and functional
572 consequences. Nat Rev Microbiol. 2019. Epub 2019/04/17. doi: 10.1038/s41579-019-0195-4.
573 PubMed PMID: 30988511.
574 6. Craig L, Pique ME, Tainer JA. Type IV pilus structure and bacterial pathogenicity. Nat
575 Rev Microbiol. 2004;2(5):363-78. doi: 10.1038/nrmicro885. PubMed PMID: 15100690.
576 7. McCallum M, Tammam S, Khan A, Burrows LL, Howell PL. The molecular mechanism of
577 the type IVa pilus motors. Nat Commun. 2017;8:15091. doi: 10.1038/ncomms15091. PubMed
578 PMID: 28474682; PubMed Central PMCID: PMCPMC5424180.
579 8. Bischof LF, Friedrich C, Harms A, Sogaard-Andersen L, van der Does C. The Type IV
580 Pilus Assembly ATPase PilB of Myxococcus xanthus Interacts with the Inner Membrane
581 Platform Protein PilC and the Nucleotide-binding Protein PilM. J Biol Chem. 2016;291(13):6946-
582 57. doi: 10.1074/jbc.M115.701284. PubMed PMID: 26851283; PubMed Central PMCID:
583 PMCPMC4807279.
584 9. Chang YW, Rettberg LA, Treuner-Lange A, Iwasa J, Sogaard-Andersen L, Jensen GJ.
585 Architecture of the type IVa pilus machine. Science. 2016;351(6278):aad2001. doi:
586 10.1126/science.aad2001. PubMed PMID: 26965631.
587 10. Chiang P, Habash M, Burrows LL. Disparate subcellular localization patterns of
588 Pseudomonas aeruginosa Type IV pilus ATPases involved in twitching motility. J Bacteriol.
589 2005;187(3):829-39. doi: 10.1128/JB.187.3.829-839.2005. PubMed PMID: 15659660; PubMed
590 Central PMCID: PMCPMC545728.
591 11. Craig L, Volkmann N, Arvai AS, Pique ME, Yeager M, Egelman EH, et al. Type IV pilus
592 structure by cryo-electron microscopy and crystallography: implications for pilus assembly and
593 functions. Mol Cell. 2006;23(5):651-62. doi: 10.1016/j.molcel.2006.07.004. PubMed PMID:
594 16949362.
595 12. Jakovljevic V, Leonardy S, Hoppert M, Sogaard-Andersen L. PilB and PilT are ATPases
596 acting antagonistically in type IV pilus function in Myxococcus xanthus. J Bacteriol.

597 2008;190(7):2411-21. doi: 10.1128/JB.01793-07. PubMed PMID: 18223089; PubMed Central
598 PMCID: PMCPMC2293208.
599 13. Whitchurch CB, Mattick JS. Characterization of a gene, pilU, required for twitching
600 motility but not phage sensitivity in Pseudomonas aeruginosa. Mol Microbiol. 1994;13(6):1079-
601 91. Epub 1994/09/01. PubMed PMID: 7854122.
602 14. Blair KM, Turner L, Winkelman JT, Berg HC, Kearns DB. A molecular clutch disables
603 flagella in the Bacillus subtilis biofilm. Science. 2008;320(5883):1636-8. doi:
604 10.1126/science.1157877. PubMed PMID: 18566286.
605 15. Ellison CK, Kan J, Dillard RS, Kysela DT, Ducret A, Berne C, et al. Obstruction of pilus
606 retraction stimulates bacterial surface sensing. Science. 2017;358(6362):535-8. doi:
607 10.1126/science.aan5706. PubMed PMID: 29074778.
608 16. Ellison CK, Dalia TN, Dalia AB, Brun YV. Real-time microscopy and physical
609 perturbation of bacterial pili using maleimide-conjugated molecules. Nat Protoc. 2019. doi:
610 10.1038/s41596-019-0162-6. PubMed PMID: 31028374.
611 17. Ellison CK, Dalia TN, Vidal Ceballos A, Wang JC, Biais N, Brun YV, et al. Retraction of
612 DNA-bound type IV competence pili initiates DNA uptake during natural transformation in Vibrio
613 cholerae. Nat Microbiol. 2018;3(7):773-80. doi: 10.1038/s41564-018-0174-y. PubMed PMID:
614 29891864.
615 18. Seitz P, Blokesch M. DNA-uptake machinery of naturally competent Vibrio cholerae.
616 Proc Natl Acad Sci U S A. 2013;110(44):17987-92. Epub 2013/10/16. doi: 1315647110 [pii]
617 10.1073/pnas.1315647110. PubMed PMID: 24127573.
618 19. Bieber D, Ramer SW, Wu CY, Murray WJ, Tobe T, Fernandez R, et al. Type IV pili,
619 transient bacterial aggregates, and virulence of enteropathogenic Escherichia coli. Science.
620 1998;280(5372):2114-8. PubMed PMID: 9641917.

621 20. Chamot-Rooke J, Mikaty G, Malosse C, Soyer M, Dumont A, Gault J, et al.
622 Posttranslational modification of pili upon cell contact triggers N. meningitidis dissemination.
623 Science. 2011;331(6018):778-82. doi: 10.1126/science.1200729. PubMed PMID: 21311024.
624 21. Helaine S, Carbonnelle E, Prouvensier L, Beretti JL, Nassif X, Pelicic V. PilX, a pilus-
625 associated protein essential for bacterial aggregation, is a key to pilus-facilitated attachment of
626 Neisseria meningitidis to human cells. Mol Microbiol. 2005;55(1):65-77. doi: 10.1111/j.1365-
627 2958.2004.04372.x. PubMed PMID: 15612917.
628 22. Adams DW, Stutzmann S, Stoudman C, Blokesch M. DNA-uptake pilus of Vibrio
629 cholerae capable of kin-discriminated auto-aggregation. bioRxiv. 2018:doi.org/10.1101/354878.
630 Epub June 26, 2018.
631 23. Dietrich M, Mollenkopf H, So M, Friedrich A. Pilin regulation in the pilT mutant of
632 Neisseria gonorrhoeae strain MS11. FEMS Microbiol Lett. 2009;296(2):248-56. doi:
633 10.1111/j.1574-6968.2009.01647.x. PubMed PMID: 19486161; PubMed Central PMCID:
634 PMCPMC4428587.
635 24. Merz AJ, So M, Sheetz MP. Pilus retraction powers bacterial twitching motility. Nature.
636 2000;407(6800):98-102. doi: 10.1038/35024105. PubMed PMID: 10993081.
637 25. Pujol C, Eugene E, Marceau M, Nassif X. The meningococcal PilT protein is required for
638 induction of intimate attachment to epithelial cells following pilus-mediated adhesion. Proc Natl
639 Acad Sci U S A. 1999;96(7):4017-22. PubMed PMID: 10097155; PubMed Central PMCID:
640 PMCPMC22412.
641 26. Hockenberry AM, Hutchens DM, Agellon A, So M. Attenuation of the Type IV Pilus
642 Retraction Motor Influences Neisseria gonorrhoeae Social and Infection Behavior. MBio.
643 2016;7(6). doi: 10.1128/mBio.01994-16. PubMed PMID: 27923924; PubMed Central PMCID:
644 PMCPMC5142622.

645 27. Wolfgang M, Lauer P, Park HS, Brossay L, Hebert J, Koomey M. PilT mutations lead to
646 simultaneous defects in competence for natural transformation and twitching motility in piliated
647 Neisseria gonorrhoeae. Mol Microbiol. 1998;29(1):321-30. PubMed PMID: 9701824.
648 28. Leighton TL, Dayalani N, Sampaleanu LM, Howell PL, Burrows LL. Novel Role for PilNO
649 in Type IV Pilus Retraction Revealed by Alignment Subcomplex Mutations. J Bacteriol.
650 2015;197(13):2229-38. doi: 10.1128/JB.00220-15. PubMed PMID: 25917913; PubMed Central
651 PMCID: PMCPMC4455263.
652 29. Aukema KG, Kron EM, Herdendorf TJ, Forest KT. Functional dissection of a conserved
653 motif within the pilus retraction protein PilT. J Bacteriol. 2005;187(2):611-8. doi:
654 10.1128/JB.187.2.611-618.2005. PubMed PMID: 15629932; PubMed Central PMCID:
655 PMCPMC543540.
656 30. Tala L, Fineberg A, Kukura P, Persat A. Pseudomonas aeruginosa orchestrates
657 twitching motility by sequential control of type IV pili movements. Nat Microbiol. 2019. Epub
658 2019/02/26. doi: 10.1038/s41564-019-0378-9. PubMed PMID: 30804544.
659 31. Biais N, Higashi D, So M, Ladoux B. Techniques to measure pilus retraction forces.
660 Methods Mol Biol. 2012;799:197-216. doi: 10.1007/978-1-61779-346-2_13. PubMed PMID:
661 21993648; PubMed Central PMCID: PMCPMC5160128.
662 32. Georgiadou M, Castagnini M, Karimova G, Ladant D, Pelicic V. Large-scale study of the
663 interactions between proteins involved in type IV pilus biology in Neisseria meningitidis:
664 characterization of a subcomplex involved in pilus assembly. Mol Microbiol. 2012;84(5):857-73.
665 doi: 10.1111/j.1365-2958.2012.08062.x. PubMed PMID: 22486968.
666 33. Karimova G, Pidoux J, Ullmann A, Ladant D. A bacterial two-hybrid system based on a
667 reconstituted signal transduction pathway. Proc Natl Acad Sci U S A. 1998;95(10):5752-6. Epub
668 1998/05/20. PubMed PMID: 9576956; PubMed Central PMCID: PMCPMC20451.
669 34. Forest KT, Satyshur KA, Worzalla GA, Hansen JK, Herdendorf TJ. The pilus-retraction
670 protein PilT: ultrastructure of the biological assembly. Acta Crystallogr D Biol Crystallogr.

671 2004;60(Pt 5):978-82. Epub 2004/04/23. doi: 10.1107/S0907444904006055. PubMed PMID:
672 15103158.
673 35. Jones CJ, Utada A, Davis KR, Thongsomboon W, Zamorano Sanchez D, Banakar V, et
674 al. C-di-GMP Regulates Motile to Sessile Transition by Modulating MshA Pili Biogenesis and
675 Near-Surface Motility Behavior in Vibrio cholerae. PLoS Pathog. 2015;11(10):e1005068. doi:
676 10.1371/journal.ppat.1005068. PubMed PMID: 26505896; PubMed Central PMCID:
677 PMCPMC4624765.
678 36. Takhar HK, Kemp K, Kim M, Howell PL, Burrows LL. The platform protein is essential for
679 type IV pilus biogenesis. J Biol Chem. 2013;288(14):9721-8. doi: 10.1074/jbc.M113.453506.
680 PubMed PMID: 23413032; PubMed Central PMCID: PMCPMC3617274.
681 37. McCallum M, Tammam S, Little DJ, Robinson H, Koo J, Shah M, et al. PilN Binding
682 Modulates the Structure and Binding Partners of the Pseudomonas aeruginosa Type IVa Pilus
683 Protein PilM. J Biol Chem. 2016;291(21):11003-15. doi: 10.1074/jbc.M116.718353. PubMed
684 PMID: 27022027; PubMed Central PMCID: PMCPMC4900251.
685 38. Zollner R, Cronenberg T, Maier B. Motor properties of PilT-independent type 4 pilus
686 retraction in gonococci. J Bacteriol. 2019. doi: 10.1128/JB.00778-18. PubMed PMID: 30692169.
687 39. Juni E, Janik A. Transformation of Acinetobacter calco-aceticus (Bacterium anitratum). J
688 Bacteriol. 1969;98(1):281-8. PubMed PMID: 5781579; PubMed Central PMCID:
689 PMCPMC249934.
690 40. Dalia AB. Natural Cotransformation and Multiplex Genome Editing by Natural
691 Transformation (MuGENT) of Vibrio cholerae. Methods Mol Biol. 2018;1839:53-64. doi:
692 10.1007/978-1-4939-8685-9_6. PubMed PMID: 30047054.
693 41. Dalia AB, McDonough E, Camilli A. Multiplex genome editing by natural transformation.
694 Proc Natl Acad Sci U S A. 2014;111(24):8937-42. doi: 10.1073/pnas.1406478111. PubMed
695 PMID: 24889608; PubMed Central PMCID: PMC4066482.

696 42. Dalia TN, Yoon SH, Galli E, Barre FX, Waters CM, Dalia AB. Enhancing multiplex
697 genome editing by natural transformation (MuGENT) via inactivation of ssDNA exonucleases.
698 Nucleic Acids Res. 2017;45(12):7527-37. doi: 10.1093/nar/gkx496. PubMed PMID: 28575400;
699 PubMed Central PMCID: PMCPMC5499599.
700 43. Dalia AB, Lazinski DW, Camilli A. Characterization of undermethylated sites in Vibrio
701 cholerae. J Bacteriol. 2013;195(10):2389-99. doi: 10.1128/JB.02112-12. PubMed PMID:
702 23504020; PubMed Central PMCID: PMC3650525.
703 44. Zhu J, Miller MB, Vance RE, Dziejman M, Bassler BL, Mekalanos JJ. Quorum-sensing
704 regulators control virulence gene expression in Vibrio cholerae. Proc Natl Acad Sci U S A.
705 2002;99(5):3129-34. Epub 2002/02/21. doi: 10.1073/pnas.052694299
706 052694299 [pii]. PubMed PMID: 11854465; PubMed Central PMCID: PMC122484.
707 45. Lo Scrudato M, Blokesch M. The regulatory network of natural competence and
708 transformation of Vibrio cholerae. PLoS Genet. 2012;8(6):e1002778. Epub 2012/06/28. doi:
709 10.1371/journal.pgen.1002778
710 PGENETICS-D-12-00108 [pii]. PubMed PMID: 22737089; PubMed Central PMCID:
711 PMC3380833.
712 46. Lo Scrudato M, Blokesch M. A transcriptional regulator linking quorum sensing and chitin
713 induction to render Vibrio cholerae naturally transformable. Nucleic Acids Res. 2013;41(6):3644-
714 58. Epub 2013/02/06. doi: gkt041 [pii]
715 10.1093/nar/gkt041. PubMed PMID: 23382174; PubMed Central PMCID: PMC3616704.
716 47. Meibom KL, Blokesch M, Dolganov NA, Wu CY, Schoolnik GK. Chitin induces natural
717 competence in Vibrio cholerae. Science. 2005;310(5755):1824-7. Epub 2005/12/17. doi:
718 310/5755/1824 [pii]
719 10.1126/science.1120096. PubMed PMID: 16357262.

720 48. Dalia AB, Lazinski DW, Camilli A. Identification of a membrane-bound transcriptional
721 regulator that links chitin and natural competence in Vibrio cholerae. MBio. 2014;5(1):e01028-
722 13. doi: 10.1128/mBio.01028-13. PubMed PMID: 24473132; PubMed Central PMCID:
723 PMC3903286.
724 49. Nero TM, Dalia TN, Wang JC, Kysela DT, Bochman ML, Dalia AB. ComM is a
725 hexameric helicase that promotes branch migration during natural transformation in diverse
726 Gram-negative species. Nucleic Acids Res. 2018;46(12):6099-111. doi: 10.1093/nar/gky343.
727 PubMed PMID: 29722872.
728 50. Ludtke SJ. Single-Particle Refinement and Variability Analysis in EMAN2.1. Methods
729 Enzymol. 2016;579:159-89. Epub 2016/08/31. doi: 10.1016/bs.mie.2016.05.001. PubMed
730 PMID: 27572727; PubMed Central PMCID: PMCPMC5101015.
731 51. Scheres SH. Semi-automated selection of cryo-EM particles in RELION-1.3. J Struct
732 Biol. 2015;189(2):114-22. Epub 2014/12/09. doi: 10.1016/j.jsb.2014.11.010. PubMed PMID:
733 25486611; PubMed Central PMCID: PMCPMC4318617.
734 52. Pettersen EF, Goddard TD, Huang CC, Couch GS, Greenblatt DM, Meng EC, et al.
735 UCSF Chimera--a visualization system for exploratory research and analysis. J Comput Chem.
736 2004;25(13):1605-12. Epub 2004/07/21. doi: 10.1002/jcc.20084. PubMed PMID: 15264254.

737

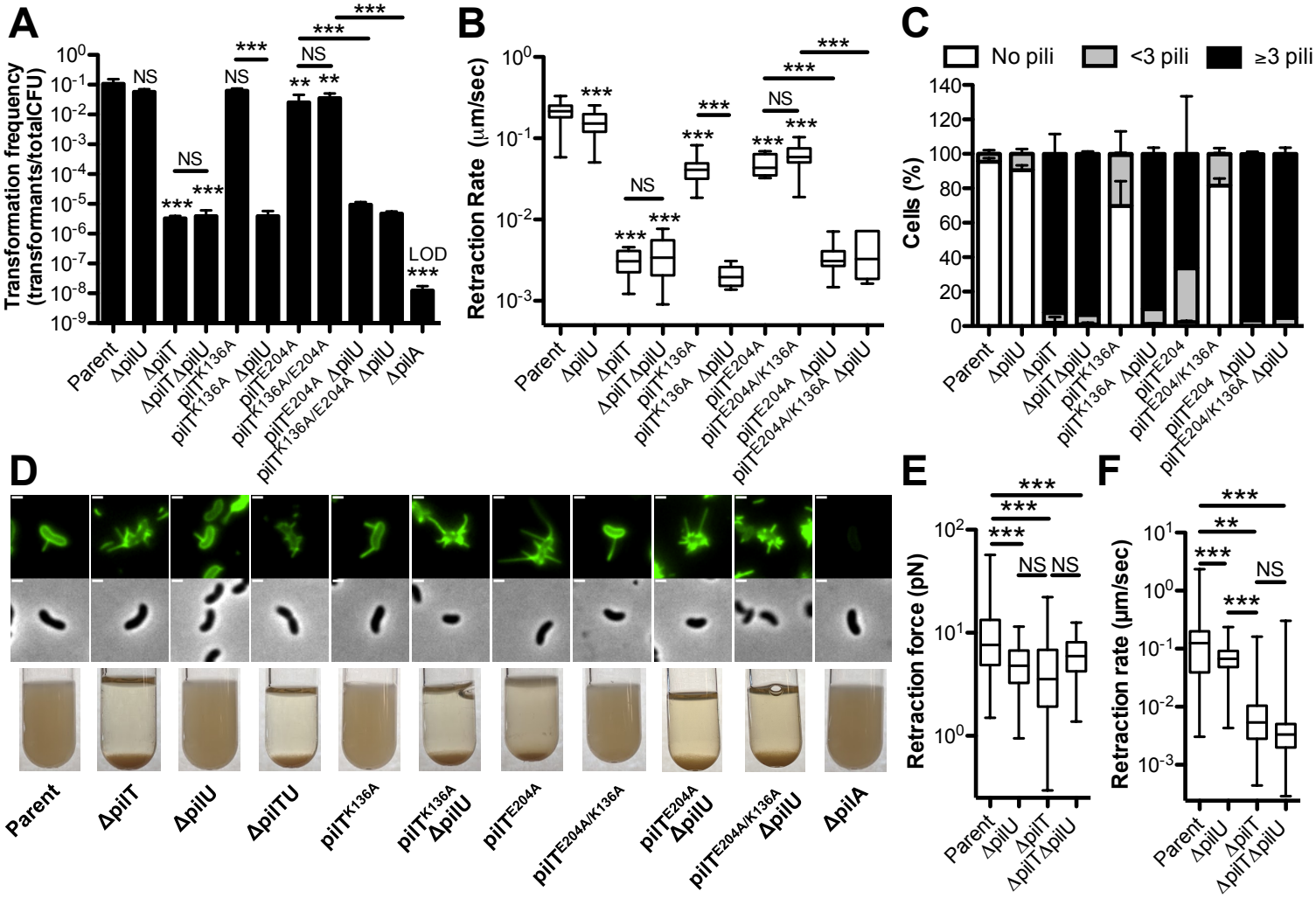

Fig 1. PilU mediates type IVa competence pilus retraction in a PilT-dependent manner in *V. cholerae*. (A) Natural transformation assays of the indicated strains. Reactions were incubated with 500 ng of transforming DNA overnight. Parent, n = 11, all other strains, n = 4. **(B)** Retraction rates of the indicated strains measured by epifluorescence time-lapse microscopy of AF488-mal labeled cells. Data are from three independent biological replicates; Parent, n = 68. Δ*pilU*, n = 56. Δ*pilT*, n = 9. Δ*pilT*Δ*pilU*, n = 18. *pilT*^{K136A}, n = 66. *pilT*^{K136A}Δ*pilU*, n = 9. *pilT*^{E204A}, n = 5. *pilT*$^{E204A/K136A}$, n = 50. *pilT*^{E204A} Δ*pilU*, n = 17. *pilT*$^{E204A/K136A}$ Δ*pilU*, n = 6. **(C)** The percentage of cells with 0, <3 or ≥3 surface pili was determined from a static image. Data are from three independent biological replicates; Parent, n = 453. Δ*pilU*, n = 413. Δ*pilT*, n = 381. Δ*pilT*Δ*pilU*, n = 425. *pilT*^{K136A}, n = 417. *pilT*^{K136A} Δ*pilU*, n = 413. *pilT*^{E204A}, n = 579. *pilT*$^{E204A/K136A}$, n = 713. *pilT*^{E204A} Δ*pilU*, n = 806. *pilT*$^{E204A/K136A}$ Δ*pilU*, n = 705. **(D)** Representative images of surface piliation (top) and aggregation phenotypes (bottom) for the indicated strains. Scale bar, 1 μm. **(E)** Retraction force (Parent, n = 101. Δ*pilU*, n = 90. Δ*pilT*, n = 372. Δ*pilT* Δ*pilU*, n = 43) and **(F)** retraction rate (Parent, n = 95. Δ*pilU*, n = 83. Δ*pilT*, n = 324. Δ*pilT* Δ*pilU*, n = 125) was measured via micropillar assays. All bar graphs are shown as the mean ± SD. All Box plots represent the median and the upper and lower quartile, while the whiskers demarcate the range. Asterisk(s) directly above bars denote comparisons to the parent strain. All comparisons were made by Student's two-tailed t-test. LOD, limit of detection; NS, not significant; ** = $P < 0.01$, *** = $P < 0.001$.

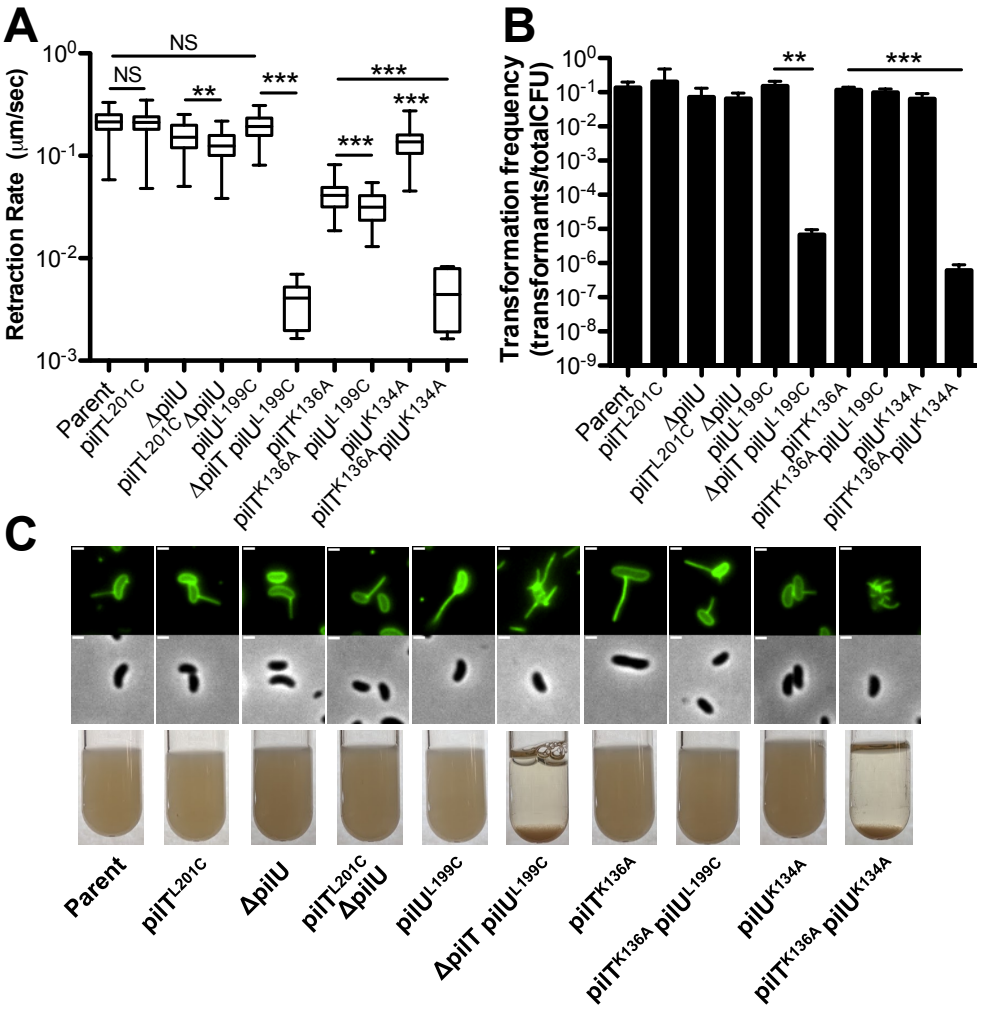

Fig 2. The ATPase activity of PilT and PilU mediate pilus retraction. (A) Retraction rates of the indicated strains measured by epifluorescence time-lapse microscopy of AF488-mal labeled cells. Box plots represent the median and the upper and lower quartile, while the whiskers demarcate the range. Data are from three independent biological replicates; *pilU*^{K134A}, *n* = 70. *pilT*^{K136A} *pilU*^{K134A}, *n* = 8. *pilT*^{K136A} *pilU*^{L199C}, *n* = 46. *pilU*^{L199C}, *n* = 49. *pilT*^{L201C}, *n* = 54. *pilT*^{L201C} Δ*pilU*, *n* = 54. Δ*pilT pilU*^{L199C}, *n* = 11. Data for the retraction rates of the parent, Δ*pilU,* and *pilT*^{K136A} strains are identical to those shown in **Fig 1B** and plotted again here to facilitate comparisons to the mutant strains indicated. **(B)** Natural transformation assays of the indicated strains incubated with 500 ng of transforming DNA overnight. Data are shown as the mean ± SD. Parent, *n* = 6. All other strains, *n* = 4**. (C)** Representative images of surface piliation (top) and aggregation phenotypes (bottom) for the indicated strains. Scale bar, 1 μm. Asterisk(s) directly above bars denote comparisons to the parent strain. All comparisons were made by Student's two-tailed t-test. NS, not significant; ** = $P < 0.01$, *** = $P < 0.001$.

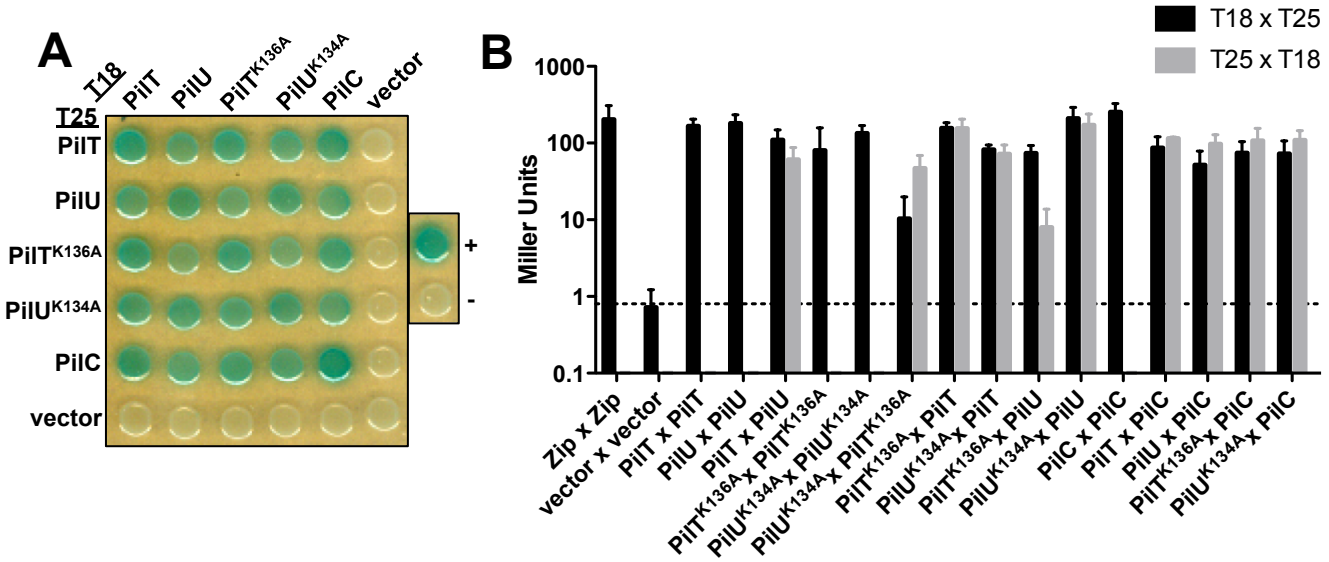

Fig 3. PilT and PilU interact with each other and the pilus platform protein PilC. Bacterial Adenylate Cyclase Two-Hybrid (BACTH) assays were performed to test pair-wise interactions between T18 and T25-tagged PilT, PilU, PilT^{K136A}, PilU^{K134A}, and PilC. Each construct was also tested for interactions with empty T18 and T25 vectors as a negative control. Leucine zipper fusions to T18 and T25 were used as the positive control (+) and empty T18 and T25 vectors served as an additional negative control (-). **(A)** Representative image of the BACTH assay plated on X-gal-containing media. **(B)** BACTH miller assays of the indicated pairwise interactions. The dotted line represents the β-galactosidase activity of the empty vector negative control. Data are shown as the mean ± SD and are from three independent experiments.

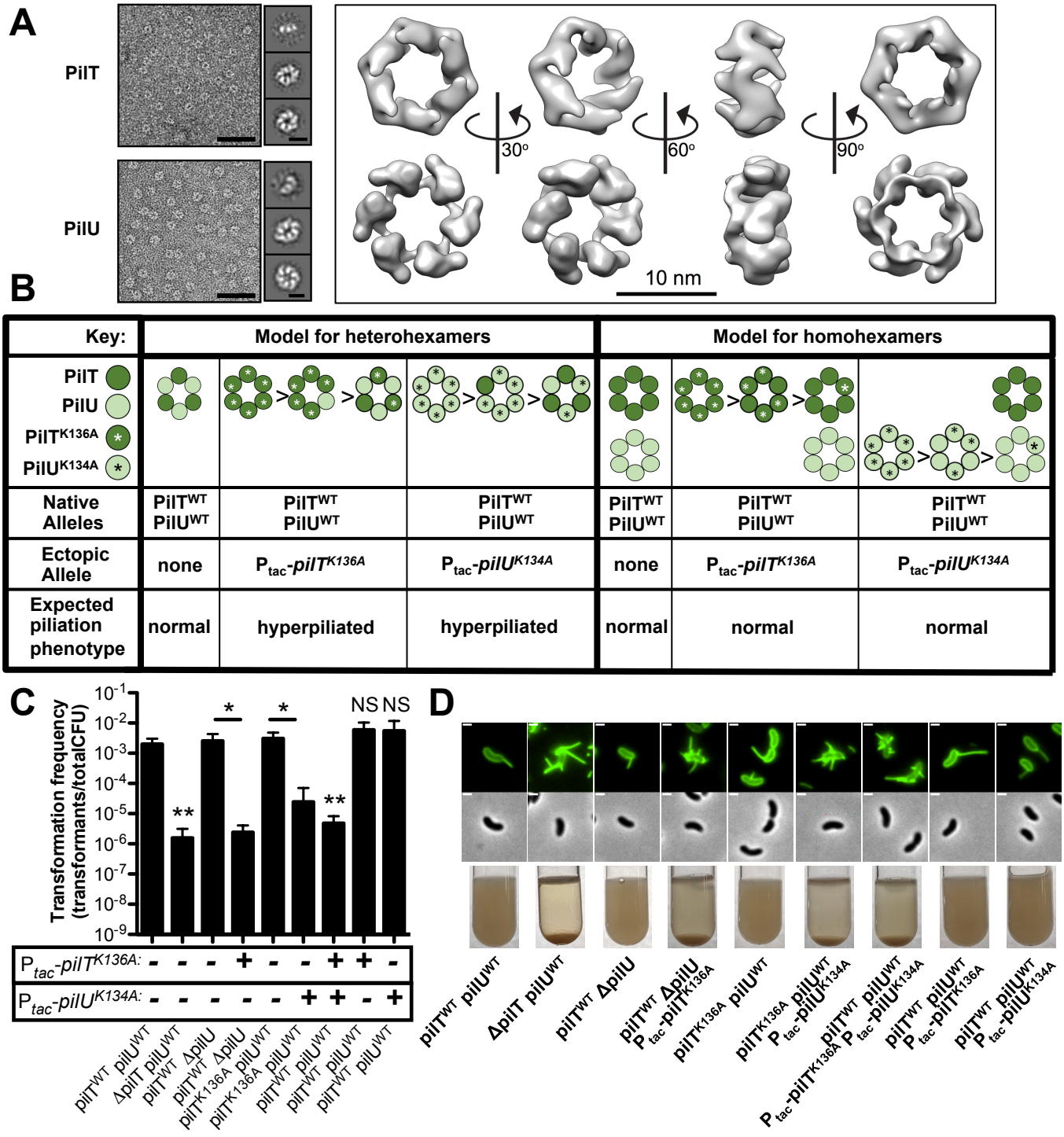

Fig 4. PilT and PilU form independent homomeric complexes *in vitro* and *in vivo* to facilitate pilus retraction. (A) Representative negative stain transmission electron micrographs of purified ^{6X}His-PilT and ^{6X}His-PilU (left; scale bar, 50 nm). 2D class averages revealing hexameric rings (middle; scale bar, 10 nm) and 3D reconstructions (right) of the ring complex imposing C6 symmetry. **(B)** Schematic of the experimental approach and expected outcomes for testing whether PilT and PilU form homomeric or heteromeric complexes to facilitate pilus retraction *in vivo*. **(C)** Natural transformation assays of indicated strains incubated with 500 ng of tDNA and after 7 minutes, DNAseI was added to prevent additional DNA uptake. The genotype of native *pilT* and *pilU* alleles are written below each bar graph and the presence or absence of a chromosomally-integrated IPTG-inducible ectopic allele of *pilT*^{K136A} or *pilU*^{K134A} is indicated by a + or -. Strains were grown with 100 μM IPTG if they contained an ectopic expression construct. Data are shown as the mean ± SD and are from four independent biological replicates. **(D)** Representative images of surface piliation (top) and aggregation phenotypes (bottom) for the indicated strains. Scale bar, 1 μm. Asterisk(s) directly above bars denote comparisons to the parent strain. All comparisons were made by Student's two-tailed t-test. NS, not significant; * = $P < 0.05$; ** = $P < 0.01$.

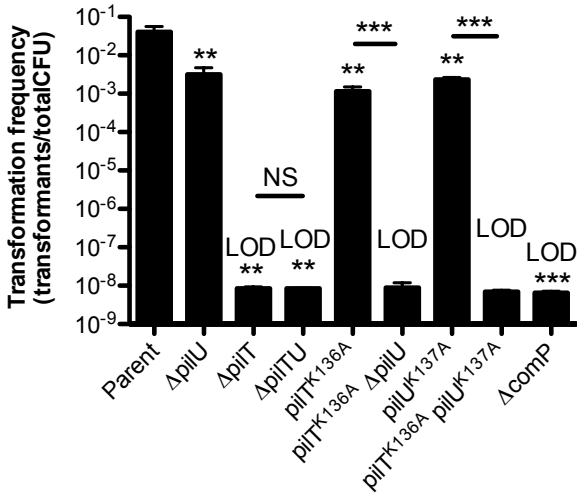

Fig 5. PilU supports pilus retraction in a PilT-dependent manner in *A. baylyi.* Natural transformation assays of the indicated strains incubated with 500ng of transforming DNA for 5 hours. Data are shown as the mean ± SD. Parent, $n = 5$. Δ*comP*, $n = 6$. All other strains, $n = 4$. Asterisk(s) directly above bars denote comparisons to parent strain. All comparisons were made by Student's two-tailed t-test. LOD, limit of detection; ** = $P < 0.01$; *** = $P < 0.001$.

Supporting Information for

PilT and PilU are homohexameric ATPases that coordinate to retract type IVa pili

Jennifer L. Chlebek[1], Hannah Q. Hughes[1], Aleksandra S. Ratkiewicz[2], Rasman Rayyan[2], Joseph Che-Yen Wang[3], Brittany E. Herrin[1], Triana N. Dalia[1], Nicolas Biais[2], and Ankur B. Dalia[1,*]

[1]Department of Biology, Indiana University, 1001 E. 3rd Street, Bloomington, IN 47405.

[2]Biology Department, CUNY Brooklyn College, 2900 Bedford Avenue, Brooklyn, NY 11210 and Graduate Center of CUNY, 365 5th Avenue, NY 10016.

[3]Electron Microscopy Center, Indiana University, Bloomington, IN 47405.

*Correspondence to: ankdalia@indiana.edu.

This PDF file includes:

S1-S4 Figs.
S1-S2 Tables

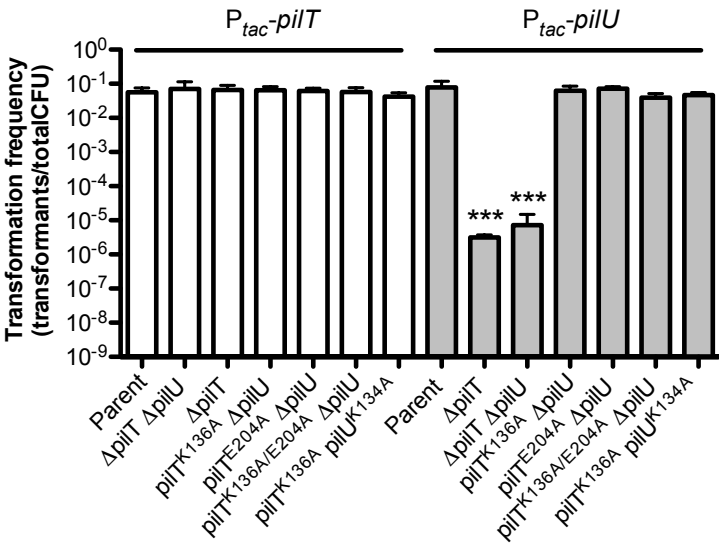

S1 Fig. Complementation analysis of *V. cholerae* mutant strains via ectopic expression of *pilT* or *pilU*. Natural transformation assays of the indicated strains. All strains contain either a chromosomally integrated IPTG-inducible P$_{tac}$-*pilT* (white bars) or P$_{tac}$-*pilU* (gray bars) construct as indicated. Data show that ectopic overexpression of PilT and PilU does not affect the transformation frequency of the parent strain. Ectopic overexpression of PilT rescued the transformation of all strains that showed a substantial reduction in natural transformation in **Fig 1A** and **Fig 2B** (i.e. Δ*pilT*, Δ*pilT* Δ*pilU*, *pilT*^{K136A} Δ*pilU*, *pilT*^{E204A} Δ*pilU*, *pilT*$^{E204A/K136A}$ Δ*pilU*, and *pilT*^{K136A} *pilU*^{K134A}). Ectopic overexpression of PilU rescued all strains except for strains that lacked a copy of *pilT* (i.e. Δ*pilT*, Δ*pilT* Δ*pilU*). All strains were grown with 100 μM IPTG to ectopically induce PilT or PilU. Data are shown as the mean ± SD. Parent, $n = 8$. All other strains, $n = 4$. Asterisk(s) directly above data denote comparisons to the parent strain. All comparisons were made by Student's two-tailed t-test. *** = $P < 0.001$.

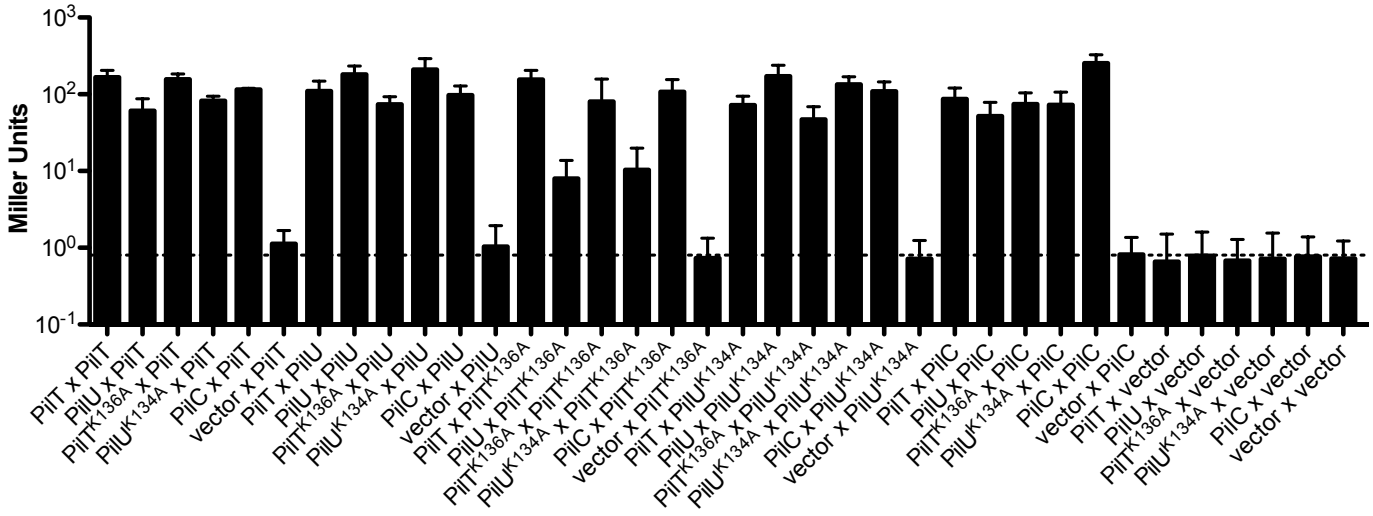

S2 Fig. PilT and PilU interact with each other and the pilus platform protein PilC. BACTH Miller assays showing all data from **Fig 3B** with additional negative controls for every T25- or T18-fusion. Data are shown as the mean ± SD from three independent experiments. The dotted line represents the β-galactosidase activity of the empty vector negative control (T18-empty x T25-empty).

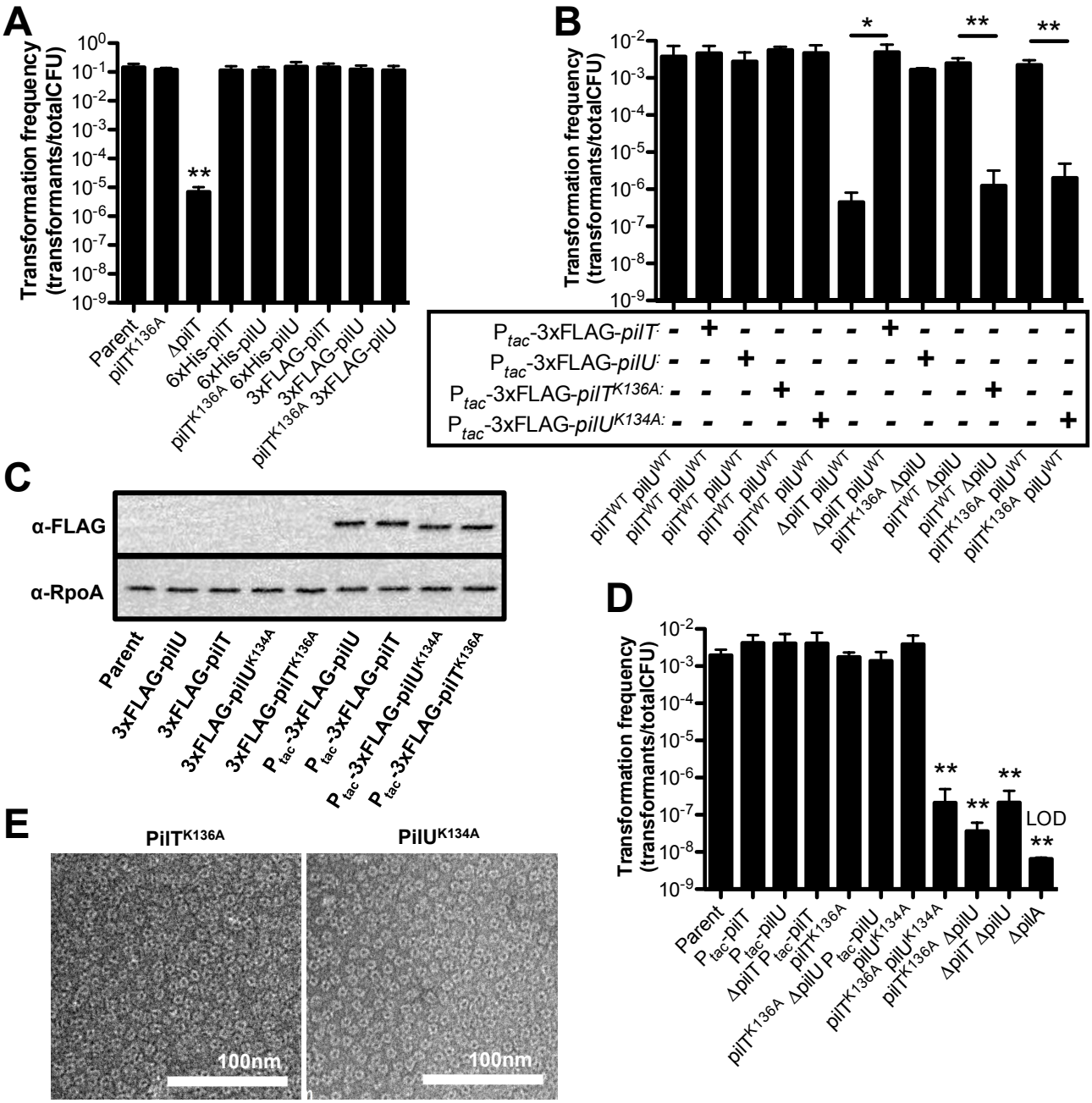

S3 Fig. PilT and PilU form homomeric complexes to facilitate pilus retraction. **(A)** Natural transformation assays showing that 6xHis and 3xFLAG N-terminal fusions to PilT and PilU are functional. The indicated strains were incubated with 500 ng of transforming DNA overnight. Parent, $n = 8$. All others, $n = 4$. **(B)** Natural transformation assays showing that overexpression of 3xFLAG tagged PilT/PilU/PilT^{K136A}/PilU^{K134A} behave the same as non-tagged proteins when ectopically overexpressed in the indicated backgrounds. Strains were incubated with 500 ng of transforming DNA and after 7 minutes, DNAse I was added to prevent additional DNA uptake. Parent, $n = 5$. *pilT^{K136A}*, $n = 5$. All others, $n = 4$. **(C)** Western blot of the indicated strains to detect FLAG tagged-proteins and RpoA as a loading control. Strains containing an IPTG regulated P_{tac} constuct were grown in the presence of 100 μM IPTG. This blot indicates that ectopic induction of 3xFLAG tagged PilT/PilU/PilT^{K136A}/PilU^{K134A} results in robust overexpression of proteins above native levels. Data is representative of three independent experiments. **(D)** Natural transformation assays where the indicated strains were incubated with 500 ng of transforming DNA for 7 minutes prior to the addition of DNAse I to prevent additional DNA uptake. These data indicate that ectopic overexpression of PilT or PilU can rescue strains with a substantial reduction in transformation frequency. All strains with P_{tac} constructs were grown with 100 μM IPTG to overexpress PilT or PilU. All bar graphs are shown as the mean ± SD. Asterisk(s) directly above bars denote comparisons to the parent strain. All comparisons were made by Student's two-tailed t-test. LOD, limit of detection; * = $P < 0.05$, ** = $P < 0.01$. **(E)** Representative negative stain transmission electron micrographs showing that purified ^{6X}His-PilT^{K136A} and ^{6X}His-PilU^{K134A} form hexamers *in vitro.* Scale bar, 100 nm.

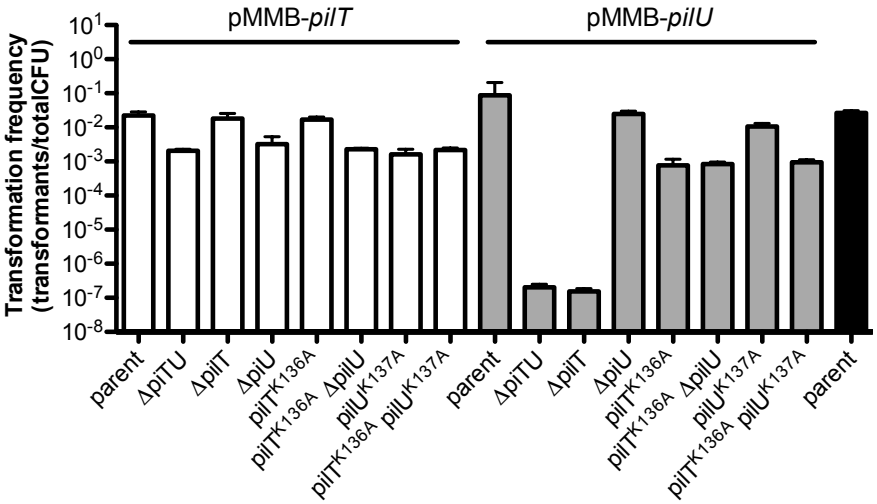

S4 Fig. Complementation analysis of *A. baylyi* mutant strains via ectopic expression of *pilT* or *pilU*. Natural transformation assays of the indicated *A. baylyi* strains. Strains harbored pMMB-*pilT* (white bars), pMMB-*pilU* (gray bars), or no vector (black bar). Data indicate that ectopic overexpression of PilT and PilU do not affect the transformation frequency of the parent strain. Ectopic overexpression of PilT rescued the transformation of all strains that showed a significant reduction in natural transformation in **Fig 5** (i.e. Δ*pilT*, Δ*pilT* Δ*pilU*, $pilT^{K136A}$ Δ*pilU*, and $pilT^{K136A}$ $pilU^{K137A}$). Ectopic overexpression of PilU rescued all strains except for strains that lacked a copy of pilT (i.e. Δ*pilT* and Δ*pilT* Δ*pilU*). All strains were grown with 100 μM IPTG to induce expression of *pilT* or *pilU*. Data are shown as the mean ± SD and are from three independent experiments.

S1 Table. Strains used in this study

Strain name in manuscript	Genotype and antibiotic resistances	Figure	Strain #
Parent	E7946 SmR, ΔlacZ::lacIq, P_{tac}-tfoX, ΔluxO::miniFRT, ΔVC1807::ZeoR, pilA S67C	Fig 1, Fig 2	TND0905 (SAD2468)
ΔpilU	E7946 SmR, ΔlacZ::lacIq, P_{tac}-tfoX, ΔluxO::SpecR, ΔVC1807::CmR, pilA S67C, comEA-mCherry, ΔpilU::TmR *	Fig 1, Fig 2	SAD2135
ΔpilT	E7946 SmR, ΔlacZ::lacIq, P_{tac}-tfoX, ΔluxO::miniFRT, ΔVC1807::ZeoR, pilA S67C, ΔpilT::TmR	Fig 1, Supp Fig 3	TND1035 (SAD2469)
ΔpilTU	E7946 SmR, ΔlacZ::lacIq, P_{tac}-tfoX, ΔluxO::miniFRT, ΔVC1807::ZeoR, pilA S67C, ΔpilTU::TmR	Fig 1	JLC227 (SAD2470)
$pilT^{K136A}$	E7946 SmR, ΔlacZ::lacIq, P_{tac}-tfoX, ΔluxO::miniFRT, ΔVC1807::KanR, pilA S67C, pilT K136A	Fig 1, Fig 2	TND1077 (SAD2471)
$pilT^{K136A}$ ΔpilU	E7946 SmR, ΔlacZ::lacIq, P_{tac}-tfoX, ΔluxO::miniFRT, ΔVC1807::ZeoR, pilA S67C, pilT K136A, ΔpilU::TmR	Fig 1	JLC444 (SAD2472)
$pilT^{E204A}$	E7946 SmR, ΔlacZ::lacIq, P_{tac}-tfoX, ΔluxO::miniFRT, ΔVC1807::CmR, pilA S67C, pilT E204A	Fig 1	TND1203 (SAD2473)
$pilT^{E204A/K136A}$	E7946 SmR, ΔlacZ::lacIq, P_{tac}-tfoX, ΔluxO::miniFRT, ΔVC1807::CmR, pilA S67C, pilT E204A/K136A	Fig 1	JLC324 (SAD2474)
$pilT^{E204A/K136A}$ ΔpilU	E7946 SmR, ΔlacZ::lacIq, P_{tac}-tfoX, ΔluxO::miniFRT, ΔVC1807::CmR, pilA S67C, pilT E204A/K136A, ΔpilU::TmR	Fig 1	JLC530 (SAD2475)
$pilT^{E204A}$ ΔpilU	E7946 SmR, ΔlacZ::lacIq, P_{tac}-tfoX, ΔluxO::miniFRT, ΔVC1807::CmR, pilA S67C, pilT E204A, ΔpilU::TmR	Fig 1	JLC531 (SAD2476)
ΔpilA	E7946 SmR, ΔlacZ::lacIq, P_{tac}-tfoX, ΔluxO::SpecR, ΔVC1807::KanR, ΔpilA::miniFRT	Fig 1	TND0855 (SAD2477)
Parent (micropillar assays)	E7946 SmR, ΔlacZ::lacIq, P_{tac}-tfoX, ΔluxO::SpecR, ΔVC1807::CmR, pilA S67C, ΔflaA::CarbR, ΔmshA::miniFRT, Δvps-rbmA::ZeoR, ΔtcpA::KanR	Fig 1	TND0752 (SAD2478)
ΔpilT (micropillar assays)	E7946 SmR, ΔlacZ::lacIq, P_{tac}-tfoX, ΔluxO::SpecR, ΔVC1807::CmR, pilA S67C, ΔflaA::CarbR, ΔmshA::miniFRT, Δvps-rbmA::ZeoR, ΔtcpA::KanR, ΔpilT::TmR	Fig 1	TND0767 (SAD2479)
ΔpilU (micropillar assays)	E7946 SmR, ΔlacZ::lacIq, P_{tac}-tfoX, ΔluxO::SpecR, ΔVC1807::CmR, pilA S67C, ΔflaA::CarbR, ΔmshA::miniFRT, Δvps-rbmA::ZeoR, ΔtcpA::KanR, ΔpilU::TmR	Fig 1	TND1168 (SAD2480)
P_{tac}-PilT	E7946 SmR, P_{tac}-tfoX, ΔluxO::miniFRT, ΔVC1807::ZeoR, pilA S67C, ΔlacZ::P_{tac}-PilT SpecR	Supp Fig 1	JLC426 (SAD2481)

P_{tac}-PilU	E7946 SmR, P_{tac}-tfoX, ΔluxO::miniFRT, ΔVC1807::ZeoR, pilA S67C, ΔlacZ::P_{tac}-PilU SpecR	Supp Fig 1	JLC427 (SAD2482)
P_{tac}-PilT ΔpilTU	E7946 SmR, P_{tac}-tfoX, ΔluxO::miniFRT, ΔVC1807::ZeoR, pilA S67C, ΔlacZ::P_{tac}-PilT SpecR, ΔpilTU::TmR	Supp Fig 1	JLC420 (SAD2483)
P_{tac}-PilU ΔpilTU	E7946 SmR, P_{tac}-tfoX, ΔluxO::miniFRT, ΔVC1807::ZeoR, pilA S67C, ΔlacZ::P_{tac}-PilU SpecR, ΔpilTU::TmR	Supp Fig 1	JLC421 (SAD2484)
P_{tac}-PilT pilT^{K136A} ΔpilU	E7946 SmR, P_{tac}-tfoX, ΔluxO::miniFRT, ΔVC1807::KanR, pilA S67C, ΔlacZ::P_{tac}-PilT SpecR, pilT K136A, ΔpilU::TmR	Supp Fig 1	JLC450 (SAD2485)
P_{tac} -PilU pilT^{K136A} ΔpilU	E7946 SmR, P_{tac}-tfoX, ΔluxO::miniFRT, ΔVC1807::KanR, pilA S67C, ΔlacZ::P_{tac}-PilU SpecR, pilT K136A, ΔpilU::TmR	Supp Fig 1	JLC451 (SAD2486)
P_{tac} -PilT pilT^{K136A} pilU^{K134A}	E7946 SmR, P_{tac}-tfoX, ΔluxO::miniFRT, ΔVC1807::KanR, pilA S67C, ΔlacZ::P_{tac}-PilT SpecR, pilT K136A pilU K134A	Supp Fig 1	JLC424 (SAD2487)
P_{tac}-PilU pilT^{K136A} pilU^{K134A}	E7946 SmR, P_{tac}-tfoX, ΔluxO::miniFRT, ΔVC1807::KanR, pilA S67C, ΔlacZ::P_{tac}-PilU SpecR, pilT K136A pilU K134A	Supp Fig 1	JLC425 (SAD2488)
P_{tac}-PilT ΔpilTU	E7946 SmR, P_{tac}-tfoX, ΔluxO::miniFRT, ΔVC1807::ZeoR, pilA S67C, ΔlacZ::P_{tac}-PilT SpecR, ΔpilTU::TmR	Supp Fig 1	JLC438 (SAD2489)
P_{tac}-PilU ΔpilTU	E7946 SmR, P_{tac}-tfoX, ΔluxO::miniFRT, ΔVC1807::ZeoR, pilA S67C, ΔlacZ::P_{tac}-PilU SpecR, ΔpilTU::TmR	Supp Fig 1	JLC439 (SAD2490)
P_{tac}-PilT pilT$^{E204A/K136A}$ ΔpilU	E7946 SmR, P_{tac}-tfoX, ΔluxO::miniFRT, ΔVC1807::CmR, pilA S67C, pilT E204A/K136A, ΔpilU::TmR, ΔlacZ::P_{tac}-PilT SpecR	Supp Fig 1	JLC540 (SAD2491)
P_{tac}-PilU pilT$^{E204A/K136A}$ ΔpilU	E7946 SmR, P_{tac}-tfoX, ΔluxO::miniFRT, ΔVC1807::CmR, pilA S67C, pilT E204A/K136A, ΔpilU::TmR, ΔlacZ::P_{tac}-PilU SpecR	Supp Fig 1	JLC541 (SAD2492)
P_{tac}-PilT pilT^{E204A} ΔpilU	E7946 SmR, P_{tac}-tfoX, ΔluxO::miniFRT, ΔVC1807::CmR, pilA S67C, pilT E204A, ΔpilU::TmR, ΔlacZ::P_{tac}-PilT SpecR	Supp Fig 1	JLC542 (SAD2493)
P_{tac}-PilU pilT^{E204A} ΔpilU	E7946 SmR, P_{tac}-tfoX, ΔluxO::miniFRT, ΔVC1807::CmR, pilA S67C, pilT E204A, ΔpilU::TmR, , ΔlacZ::P_{tac}-PilU SpecR	Supp Fig 1	JLC543 (SAD2494)
PilU^{L199C}	E7946 SmR, ΔlacZ::lacIq, P_{tac}-tfoX, ΔluxO::miniFRT, ΔVC1807::CmR, pilA S67C, pilU L199C	Fig 2	JLC409 (SAD2495)
ΔpilT PilU^{L199C}	E7946 SmR, ΔlacZ::lacIq, P_{tac}-tfoX, ΔluxO::miniFRT, ΔVC1807::ZeoR, pilA S67C, ΔpilT::TmR, pilU L199C	Fig 2	JLC411 (SAD2496)
pilT^{K136A} pilU^{L199C}	E7946 SmR, ΔlacZ::lacIq, P_{tac}-tfoX, ΔluxO::miniFRT, ΔVC1807::CmR, pilA S67C, pilU L199C, pilT K136A	Fig 2	JLC414 (SAD2497)

pilT^{L201C}	E7946 SmR, ΔlacZ::lacIq, P_{tac}-tfoX, ΔluxO::SpecR, ΔVC1807::CmR, pilA S67C, comEA-mCherry, pilT L201C *	Fig 2	TND0989 (SAD2498)
pilT^{L201C} ΔpilU	E7946 SmR, ΔlacZ::lacIq, P_{tac}-tfoX, ΔluxO::SpecR, ΔVC1807::CmR, pilA S67C, comEA-mCherry, pilT L201C, ΔpilU::TmR *	Fig 2	TND1140 (SAD2499)
pilU^{K134A}	E7946 SmR, ΔlacZ::lacIq, P_{tac}-tfoX, ΔluxO::miniFRT, ΔVC1807::KanR, pilA S67C, pilU K134A	Fig 2	TND1092 (SAD2500)
pilT^{K136A} pilU^{K134A}	E7946 SmR, ΔlacZ::lacIq, P_{tac}-tfoX, ΔluxO::miniFRT, ΔVC1807::KanR, pilA S67C, pilT K136A, pilU K134A	Fig 2	TND1094 (SAD2501)
^{6X}His-pilU, pilT^{K136A}	E7946 SmR, ΔlacZ::lacIq, P_{tac}-tfoX, ΔluxO::miniFRT, ΔVC1807::CmR, pilA S67C, ^{6X}His-pilU, pilT K136A	Supp Fig 3	JLC298 (SAD2502)
^{6X}His-pilT	E7946 SmR, ΔlacZ::lacIq, P_{tac}-tfoX, ΔluxO::miniFRT, ΔVC1807::CmR, pilA S67C, ^{6X}His-pilT	Supp Fig 3	HKQ046 (SAD2503)
^{6X}His-pilU	E7946 SmR, ΔlacZ::lacIq, P_{tac}-tfoX, ΔluxO::miniFRT, ΔVC1807::CmR, pilA S67C, ^{6X}His-pilU	Supp Fig 3	JLC398 (SAD2504)
pilT^{K136A} 3xFLAG-pilU	E7946 SmR, ΔlacZ::lacIq, P_{tac}-tfoX, ΔluxO::miniFRT, ΔVC1807::CmR, pilA S67C, pilT K136A, 3xFLAG-pilU	Supp Fig 3	JLC396 (SAD2505)
3xFLAG-pilU	E7946 SmR, ΔlacZ::lacIq, P_{tac}-tfoX, ΔluxO::miniFRT, ΔVC1807::CmR, pilA S67C, 3xFLAG-pilU	Supp Fig 3	JLC326 (SAD2506)
3xFLAG-pilU^{K134A}	E7946 SmR, ΔlacZ::lacIq, P_{tac}-tfoX, ΔluxO::miniFRT, ΔVC1807::CmR, pilA S67C, 3xFLAG-pilU^{K134A}	Supp Fig 3	JLC316 (SAD2507)
3xFLAG-pilT	E7946 SmR, ΔlacZ::lacIq, P_{tac}-tfoX, ΔluxO::miniFRT, ΔVC1807::CmR, pilA S67C, 3xFLAG-pilT	Supp Fig 3	JLC310 (SAD2508)
3xFLAG-pilT^{K136A}	E7946 SmR, ΔlacZ::lacIq, P_{tac}-tfoX, ΔluxO::miniFRT, ΔVC1807::CmR, pilA S67C, 3xFLAG-pilT K136A	Supp Fig 3	JLC349 (SAD2509)
^{6X}His-pilU (purification)	BL21 DE3 pHisTev-6xHis-pilU	Fig 4	HKQ051 (SAD2510)
^{6X}His-pilU^{K134A} (purification)	BL21 DE3 pHisTev-6xHis-pilU K134A	Supp Fig 3	SAD2316
^{6X}His-pilT (purification)	BL21 DE3 pHisTev-6xHis-pilT	Fig 4	TND1277 (SAD2511)
^{6X}His-pilT^{K136A} (purification)	BL21 DE3 pHisTev-6xHis-pilT K136A	Supp Fig 3	TND1281 (SAD2512)
PilT x PilT	BTH101 pUT18C-PilT (CarbR), pKT25-PilT (KanR)	Fig 3, Supp Fig 2	JLC465
PilU x PilT	BTH101 pUT18C-PilU (CarbR), pKT25-PilT (KanR)	Fig 3, Supp Fig 2	JLC466

PilT^{K136A} x PilT	BTH101 pUT18C-PilT K136A (CarbR), pKT25-PilT (KanR)	Fig 3, Supp Fig 2	JLC467
PilU^{K134A} x PilT	BTH101 pUT18C-PilU K134A (CarbR), pKT25-PilT (KanR)	Fig 3, Supp Fig 2	JLC468
PilC x PilT	BTH101 pUT18C-PilC (CarbR), pKT25-PilT (KanR)	Fig 3, Supp Fig 2	JLC469
vector x PilT	BTH101 pUT18C-vector (CarbR), pKT25-PilT (KanR)	Fig 3, Supp Fig 2	JLC470
PilT x PilU	BTH101 pUT18C-PilT (CarbR), pKT25-PilU (KanR)	Fig 3, Supp Fig 2	JLC471
PilU x PilU	BTH101 pUT18C-PilU (CarbR), pKT25-PilU (KanR)	Fig 3, Supp Fig 2	JLC472
PilT^{K136A} x PilU	BTH101 pUT18C-PilT K136A (CarbR), pKT25-PilU (KanR)	Fig 3, Supp Fig 2	JLC473
PilU^{K134A} x PilU	BTH101 pUT18C-PilU K134A (CarbR), pKT25-PilU (KanR)	Fig 3, Supp Fig 2	JLC474
PilC x PilU	BTH101 pUT18C-PilC (CarbR), pKT25-PilU (KanR)	Fig 3, Supp Fig 2	JLC475
vector x PilU	BTH101 pUT18C-vector (CarbR), pKT25-PilU (KanR)	Fig 3, Supp Fig 2	JLC476
PilT x PilT^{K136A}	BTH101 pUT18C-PilT (CarbR), pKT25-PilT K136A (KanR)	Fig 3, Supp Fig 2	JLC477
PilU x PilT^{K136A}	BTH101 pUT18C-PilU (CarbR), pKT25-PilT K136A (KanR)	Fig 3, Supp Fig 2	JLC478
PilT^{K136A} x PilT^{K136A}	BTH101 pUT18C-PilT K136A (CarbR), pKT25-PilT K136A (KanR)	Fig 3, Supp Fig 2	JLC479
PilU^{K134A} x PilT^{K136A}	BTH101 pUT18C-PilU K134A (CarbR), pKT25-PilT K136A (KanR)	Fig 3, Supp Fig 2	JLC480
PilC x PilT^{K136A}	BTH101 pUT18C-PilC (CarbR), pKT25-PilT K136A (KanR)	Fig 3, Supp Fig 2	JLC481
vector x PilT^{K136A}	BTH101 pUT18C-vector (CarbR), pKT25-PilT K136A (KanR)	Fig 3, Supp Fig 2	JLC482

PilT x PilU^{K134A}	BTH101 pUT18C-PilT (CarbR), pKT25-PilU K134A (KanR)	Fig 3, Supp Fig 2	JLC483
PilU x PilU^{K134A}	BTH101 pUT18C-PilU (CarbR), pKT25-PilU K134A (KanR)	Fig 3, Supp Fig 2	JLC484
PilT^{K136A} x PilU^{K134A}	BTH101 pUT18C-PilT K136A (CarbR), pKT25-PilU K134A (KanR)	Fig 3, Supp Fig 2	JLC485
PilU^{K134A} x PilU^{K134A}	BTH101 pUT18C-PilU K134A (CarbR), pKT25-PilU K134A (KanR)	Fig 3, Supp Fig 2	JLC486
PilC x PilU^{K134A}	BTH101 pUT18C-PilC (CarbR), pKT25-PilU K134A (KanR)	Fig 3, Supp Fig 2	JLC487
vector x PilU^{K134A}	BTH101 pUT18C-vector (CarbR), pKT25-PilU K134A (KanR)	Fig 3, Supp Fig 2	JLC488
PilT x PilC	BTH101 pUT18C-PilT (CarbR), pKT25-PilC (KanR)	Fig 3, Supp Fig 2	JLC489
PilU x PilC	BTH101 pUT18C-PilU (CarbR), pKT25-PilC (KanR)	Fig 3, Supp Fig 2	JLC490
PilT^{K136A} x PilC	BTH101 pUT18C-PilT K136A (CarbR), pKT25-PilC (KanR)	Fig 3, Supp Fig 2	JLC491
PilU^{K134A} x PilC	BTH101 pUT18C-PilU K134A (CarbR), pKT25-PilC (KanR)	Fig 3, Supp Fig 2	JLC492
PilC x PilC	BTH101 pUT18C-PilC (CarbR), pKT25-PilC (KanR)	Fig 3, Supp Fig 2	JLC493
vector x PilC	BTH101 pUT18C-vector (CarbR), pKT25-PilC (KanR)	Fig 3, Supp Fig 2	JLC494
PilT x vector	BTH101 pUT18C-PilT (CarbR), pKT25-vector (KanR)	Fig 3, Supp Fig 2	JLC495
PilU x vector	BTH101 pUT18C-PilU (CarbR), pKT25-vector (KanR)	Fig 3, Supp Fig 2	JLC496
PilT^{K136A} x vector	BTH101 pUT18C-PilT K136A (CarbR), pKT25-vector (KanR)	Fig 3, Supp Fig 2	JLC497
PilU^{K134A} x vector	BTH101 pUT18C-PilU K134A (CarbR), pKT25-vector (KanR)	Fig 3, Supp Fig 2	JLC498

PilC x vector	BTH101 pUT18C-PilC (CarbR), pKT25-vector (KanR)	Fig 3, Supp Fig 2	JLC499
vector x vector	BTH101 pUT18C-vector (CarbR), pKT25-vector (KanR)	Fig 3, Supp Fig 2	JLC500
Zip x Zip	BTH101 pUT18C-Leucine Zipper (CarbR), pKT25-Leucine Zipper (KanR)	Fig 3, Supp Fig 2	JLC501
Parent (P_{const}-tfoX)	E7946 SmR, ΔlacZ::lacIq, P_{const}-tfoX, ΔluxO::miniFRT, ΔVC1807::KanR, pilA S67C	Fig 4, Supp Fig 3	TND1076 (SAD2513)
ΔpilU	E7946 SmR, ΔlacZ::lacIq, P_{const}-tfoX, ΔluxO::miniFRT, ΔVC1807::KanR, pilA S67C, ΔpilU::TmR	Fig 4, Supp Fig 3	JLC251 (SAD2514)
ΔpilT	E7946 SmR, ΔlacZ::lacIq, P_{const}-tfoX, ΔluxO::miniFRT, ΔVC1807::KanR, pilA S67C, ΔpilT::TmR	Fig 4, Supp Fig 3	JLC250 (SAD2515)
$pilT^{K136A}$	E7946 SmR, ΔlacZ::lacIq, P_{const}-tfoX, ΔluxO::miniFRT, ΔVC1807::CmR, pilA S67C, pilT K136A	Fig 4	JLC299 (SAD2516)
P_{tac}-$pilT^{K136A}$	E7946 SmR, P_{const}-tfoX, ΔluxO::miniFRT, ΔVC1807::KanR, pilA S67C, ΔlacZ::P_{tac} -pilT K136A SpecR	Fig 4	JLC277 (SAD2517)
ΔpilU P_{tac}-$pilT^{K136A}$	E7946 SmR, P_{const}-tfoX, ΔluxO::miniFRT, ΔVC1807::KanR, pilA S67C, ΔpilU::TmR, ΔlacZ::Ptac-pilT K136A SpecR	Fig 4	SAD2243
P_{tac}-$pilU^{K134A}$	E7946 SmR, P_{const}-tfoX, ΔluxO::miniFRT, ΔVC1807::KanR, pilA S67C, ΔlacZ::P_{tac}-pilU K134A SpecR	Fig 4	JLC282 (SAD2518)
$pilT^{K136A}$ P_{tac}-$pilU^{K134A}$	E7946 SmR, P_{const}-tfoX, ΔluxO::miniFRT, ΔVC1807::CmR, pilA S67C, ΔlacZ::P_{tac}-pilU K134A SpecR, pilT K136A	Fig 4	JLC300 (SAD2519)
P_{tac}-$pilT^{K136A}$ P_{tac}-$pilU^{K134A}$	E7946 SmR, P_{const}-tfoX, ΔluxO::miniFRT, pilA S67C, ΔlacZ::P_{tac}-pilU K134A SpecR, ΔVC1807::Ptac-pilT K136A CmR	Fig 4	SAD2242
P_{tac}-3xFLAG-PilU	E7946 SmR, P_{const}-tfoX, ΔluxO::miniFRT, ΔVC1807::KanR, pilA S67C, ΔlacZ::P_{tac}-3xFLAG-pilU SpecR	Supp Fig 3	JLC333 (SAD2520)
P_{tac}-3x FLAG-PilU K134A	E7946 SmR, P_{const}-tfoX, ΔluxO::miniFRT, ΔVC1807::KanR, pilA S67C, ΔlacZ::P_{tac}-3xFLAG-pilU K134A SpecR	Supp Fig 3	JLC336 (SAD2521)
P_{tac}-3x FLAG-PilT	E7946 SmR, ΔlacZ::lacIq, P_{const}-tfoX, ΔluxO::miniFRT, ΔVC1807::KanR, pilA S67C, ΔlacZ::P_{tac}-3xFLAG-pilT SpecR	Supp Fig 3	JLC337 (SAD2522)
P_{tac}-3x FLAG-$PilT^{K136A}$	E7946 SmR, P_{const}-tfoX, ΔluxO::miniFRT, ΔVC1807::KanR, pilA S67C, ΔlacZ::P_{tac}-3xFLAG-pilT K136A SpecR	Supp Fig 3	JLC353 (SAD2523)
ΔpilA	E7946 SmR, ΔlacZ::lacIq, P_{const}-tfoX, ΔluxO::miniFRT, ΔVC1807::TmR, ΔpilA::miniFRT	Supp Fig 3	TND1357 (SAD2524)

ΔpilTU	E7946 SmR, ΔlacZ::lacIq, P_{const}-tfoX, ΔluxO::miniFRT, ΔVC1807::KanR, pilA S67C, ΔpilTU::TmR	Supp Fig 3	JLC252 (SAD2525)
pilU^{K134A}	E7946 SmR, ΔlacZ::lacIq, P_{const}-tfoX, ΔluxO::miniFRT, ΔVC1807::CmR, pilA S67C, pilU K134A	Supp Fig 3	JLC308 (SAD2526)
pilT^{K136A} ΔpilU	E7946 SmR, ΔlacZ::lacIq, P_{const}-tfoX, ΔluxO::miniFRT, ΔVC1807::KanR, pilA S67C, pilT K136A, ΔpilU::TmR	Supp Fig 3	JLC447 (SAD2527)
pilT^{K136A} pilU^{K134A}	E7946 SmR, ΔlacZ::lacIq, P_{const}-tfoX, ΔluxO::miniFRT, ΔVC1807::KanR, pilA S67C, pilT K136A, pilU K134A	Supp Fig 3	JLC307 (SAD2528)
P_{tac}-pilT	E7946 SmR, P_{const}-tfoX, ΔluxO::miniFRT, ΔVC1807::KanR, pilA S67C, ΔlacZ::P_{tac}-pilT SpecR	Supp Fig 3	JLC279 (SAD2529)
ΔpilT P_{tac}-pilT	E7946 SmR, P_{const}-tfoX, ΔluxO::miniFRT, ΔVC1807::KanR, pilA S67C, ΔlacZ::P_{tac}-pilT SpecR, ΔpilT::TmR	Supp Fig 3	JLC280 (SAD2530)
P_{tac}-pilU	E7946 SmR, P_{const}-tfoX, ΔluxO::miniFRT, ΔVC1807::KanR, pilA S67C, ΔlacZ::P_{tac}-pilU SpecR	Supp Fig 3	JLC283 (SAD2531)
pilT^{K136A} ΔpilU P_{tac}-pilU	E7946 SmR, P_{const}-tfoX, ΔluxO::miniFRT, ΔVC1807::KanR, pilA S67C, ΔlacZ::P_{tac}-pilU SpecR, pilT K136A, ΔpilU::TmR	Supp Fig 3	JLC449 (SAD2532)
ΔpilT P_{tac}-3xFLAG-pilT	E7946 SmR, P_{const}-tfoX, ΔluxO::miniFRT, ΔVC1807::KanR, pilA S67C, ΔlacZ::P_{tac}-3x-FLAG-pilT SpecR, ΔpilT::TmR	Supp Fig 3	JLC373 (SAD2533)
pilT^{K136A} ΔpilU P_{tac}-3x FLAG-pilU	E7946 SmR, P_{const}-tfoX, ΔluxO::miniFRT, ΔVC1807::KanR, pilA S67C, ΔlacZ::P_{tac}-3x-FLAG-pilU SpecR, pilT K136A, ΔpilU::TmR	Supp Fig 3	JLC448 (SAD2534)
ΔpilU P_{tac}-3x FLAG-PilT^{K136A}	E7946 SmR, P_{const}-tfoX, ΔluxO::miniFRT, ΔVC1807::KanR, pilA S67C, ΔlacZ::P_{tac}-3xFLAG-pilT K136A SpecR, ΔpilU::TmR	Supp Fig 3	JLC379 (SAD2535)
pilT^{K136A} P_{tac}-3x FLAG-pilU^{K134A}	E7946 SmR, P_{const}-tfoX, ΔluxO::miniFRT, ΔVC1807::KanR, pilA S67C, ΔlacZ::P_{tac}-3x-FLAG-pilU K134A SpecR, pilT K136A	Supp Fig 3	JLC380 (SAD2536)
Parent (*A. baylyi*)	ADP1, comP T129C	Fig 5	TND0428 (SAD2537)
PilT^{K136A} ΔpilU	ADP1, comP T129C, PilT K136A ΔpilU::ZeoR	Fig 5	TND1135 (SAD2538)
PilT^{K136A} PilU^{K137A}	ADP1, , comP T129C, PilT K136A PilU K137A	Fig 5	TND1142 (SAD2539)
PilT^{K136A}	ADP1, comP T129C, PilT K136A	Fig 5	TND1122 (SAD2540)
PilU^{K137A}	ADP1, comP T129C, PilU K137A	Fig 5	TND1111 (SAD2541)
ΔpilT	ADP1, comP T129C, ΔpilT::SpecR	Fig 5	TND0779 (SAD2542)
ΔpilU	ADP1, comP T129C, ΔpilU::ZeoR	Fig 5	TND0798 (SAD2543)

ΔpilTU	ADP1, comP T129C, ΔpilTU::ZeoR	Fig 5	TND0799 (SAD2544)
ΔcomP	ADP1, ΔcomP::SpecR	Fig 5	TND0115 (SAD2545)
P_{tac}-pilT	ADP1, comP T129C, pMMB67EH- P_{tac}-pilT	Supp Fig 4	TND1703 (SAD2546)
P_{tac}-pilT ΔpilTU	ADP1, comP T129C, pMMB67EH- P_{tac}-pilT, ΔpilTU::ZeoR	Supp Fig 4	TND1704 (SAD2547)
P_{tac}-pilT ΔpilT	ADP1, comP T129C, pMMB67EH- P_{tac}-pilT, ΔpilT::SpecR	Supp Fig 4	TND1705 (SAD2548)
P_{tac}-pilT ΔpilU	ADP1, comP T129C, pMMB67EH- P_{tac}-pilT, ΔpilU::ZeoR	Supp Fig 4	TND1706 (SAD2549)
P_{tac}-pilT $pilT^{K136A}$	ADP1, comP T129C, pMMB67EH- P_{tac}-pilT, pilT K136A	Supp Fig 4	TND1707 (SAD2550)
P_{tac}-pilT $pilT^{K136A}$ ΔpilU	ADP1, comP T129C, pMMB67EH- P_{tac}-pilT, pilT K136A, ΔpilU::ZeoR	Supp Fig 4	TND1708 (SAD2551)
P_{tac}-pilT $pilU^{K137A}$	ADP1, comP T129C, pMMB67EH- P_{tac}-pilT, pilU K137A	Supp Fig 4	TND1709 (SAD2552)
P_{tac}-pilT $pilT^{K136A}$ $pilU^{K137A}$	ADP1, comP T129C, pMMB67EH- P_{tac}-pilT, pilT K136A, pilU K137A	Supp Fig 4	TND1710 (SAD2553)
P_{tac}-pilU	ADP1, comP T129C, pMMB67EH- P_{tac}-pilU	Supp Fig 4	TND1711 (SAD2554)
P_{tac}-pilU ΔpilTU	ADP1, comP T129C, pMMB67EH- P_{tac}-pilU, ΔpilTU::ZeoR	Supp Fig 4	TND1712 (SAD2555)
P_{tac}-pilU ΔpilT	ADP1, comP T129C, pMMB67EH- P_{tac}-pilU, ΔpilT::SpecR	Supp Fig 4	TND1713 (SAD2556)
P_{tac}-pilU ΔpilU	ADP1, comP T129C, pMMB67EH- P_{tac}-pilU, ΔpilU::ZeoR	Supp Fig 4	TND1714 (SAD2557)
P_{tac}-pilU $pilT^{K136A}$	ADP1, comP T129C, pMMB67EH- P_{tac}-pilU, pilT K136A	Supp Fig 4	TND1715 (SAD2558)
P_{tac}-pilU $pilT^{K136A}$ ΔpilU	ADP1, comP T129C, pMMB67EH- P_{tac}-pilU, pilT K136A, ΔpilU::ZeoR	Supp Fig 4	TND1716 (SAD2559)
P_{tac}-pilU $pilU^{K137A}$	ADP1, comP T129C, pMMB67EH- P_{tac}-pilU, pilU K137A	Supp Fig 4	TND1717 (SAD2560)
P_{tac}-pilU $pilT^{K136A}$ $pilU^{K137A}$	ADP1, comP T129C, pMMB67EH- P_{tac}-pilU, pilT K136A, pilU K137A	Supp Fig 4	TND1718 (SAD2561)

* comEA-mCherry does not affect natural transformation or retraction rates [17].

S2 Table. Primers used in this study

Primer name	Sequence (5' –> 3')	Description
BBC374	TGGCAAAAAGCGAGAGAAGAAG	ΔluxO F1
BBC375	gtcgacggatccccggaatCATGAGGACATATTTTGTTTTCTGC	ΔluxO R1
BBC376	gaagcagctccagcctacaTAAGCGATGAGAGAATGGATCAAC	ΔluxO F2
BBC377	TCACACCCGAATTTCCATCATGC	ΔluxO R2
ABD344	GATTAGCAACGATTCTAGCGCAGGAG	ΔVC1807 F1
ABD340	gtcgacggatccccggaatACGTTTCATTAGTCACCTCTATTGT TAACTTGTTC	ΔVC1807 R1
ABD341	gaagcagctccagcctacaTAGTCGAAAATAAAAAAAAGAGG CTCGCCTC	ΔVC1807 F2
ABD345	CTTGCTAACCGTTGGTGTTACCAGC	ΔVC1807 R2
pilA S81C F	AAAACTAATATTGAAGATTATATTGCGACAGAAGGC TgTTTTCCTGCAACAACTGCAGG	pilA S67C F
pilA R2	CATTAATCGCGGTTTCAAAGTGCA	pilA S67C R2
DOG0400	ACTTCTGGCTGAAGGTCAATTTTC	ΔpilT/U F1
DOG0401	gtcgacggatccccggaatCATTTAAATTCCTTAATAAAGTCTG GC	ΔpilT R1
DOG0402	gaagcagctccagcctacaTAGGTAGGTAAAGACAGATGGAG	ΔpilT F2
DOG0403	TCACGTGTTCGGCCAAAATC	ΔpilT/U R2
HQP0001	GGGCTCGGGTgctTCGACGACCTTGGCG	PilT K136A R1
HQP0002	CGCCAAGGTCGTCGAagcACCCGAGCCC	PilT K136A F2
BBC2508	GTTTCTTGGTCACGCAGagCACCGACGAGGATCAC	PilT E204A R1
BBC2509	GTGATCCTCGTCGGTGctCTGCGTGACCAAGAAAC	PilT E204A F2
BBC401	ACCAGCAAAGCTAATAAAATCGAG	ΔpilA F1
BBC402	gtcgacggatccccggaatGAGCATATGCCTTGCTACACAAG	ΔpilA R1
BBC403	gaagcagctccagcctacaACTGCAGGTGCAACAATTAACTAA	ΔpilA F2
BBC404	CGCCATACTAACCCAATACACTC	ΔpilA R2
BBC1752	CTGAATGATTTCCATGAGACG	ΔflaA F1
BBC1753	gtcgacggatccccggaatCATAGTTTGCTCTCCTATCGAG	ΔflaA R1
BBC1754	gaagcagctccagcctacaTTGCAGTAGTTCACGGTACCTTC	ΔflaA F2
BBC1755	TTATACGCTCTTTTGCGTGATGG	ΔflaA R2
BBC1450	CACTCAACGAGCTCAATACG	ΔmshA F1
ABD653	gtcgacggatccccggaatCATCTCTCTTTCATGTGAATACGCA GC	ΔmshA R1
ABD654	gaagcagctccagcctacaGCGCAATAATTTAAATATGGCTCG TGC	ΔmshA F2

BBC1453	ATAGCCTTGCTGTTCATTTTGG	ΔmshA R2
BBC2022	TGCCGATCTCGTTTATGGACG	Δvps-rbmA locus F1
BBC2023	gtcgacggatccccggaatTGCCATTTTGATTGCCTCTGG	Δvps-rbmA locus R1
BBC2024	gaagcagctccagcctacaCAAAGAGAGCCTTATTAGGCTCTC	Δvps-rbmA locus F2
BBC2025	TGAAAGAGGTTGCTCTAGAACTCG	Δvps-rbmA locus R2
BBC1457	TTTCAAGACTTTGGGCAATAG	ΔtcpA F1
BBC1968	gtcgacggatccccggaatCTGTTTTAATAATTGCATATTTATA TAACTCCACC	ΔtcpA R1
BBC1969	gaagcagctccagcctacaTTTGGTAACAGTTAATCTACACCAT TATCTTG	ΔtcpA F2
BBC1463	TTGAATTCGTCCATCATCTAAG	ΔtcpA R2
BBC1833	GATATCCATGTCCATGTCCCAG	comEA-mCherry F1
BBC1834	cttgctcactccaccacttccacctgcTAACAAGATCCTTGCGGCATTG	comEA-mCherry R1
BBC1837	acgagctgtacaagtaaGCTGCAATCATGTGTCTCG	comEA-mCherry F2
BBC1838	GTCTTTCTATCAGTTCGGACTTAGTC	comEA-mCherry R2
BBC1835	gcaggtggaagtggtggaGTGAGCAAGGGCGAGGAGG	mCherry (for comEAmCherry) F
BBC1836	gattgcagcTTACTTGTACAGCTCGTCC	mCherry (for comEAmCherry) R
DOG0405	gtcgacggatccccggaatCATCTGTCTTTACCTACCTAAAATGC	ΔpilU R1
DOG0406	gaagcagctccagcctacaTAGCGATGGTTACTTTGTGCG	ΔpilU F2
JCP048	CAAGCCCCCGATATGATTTgcATTGGTGAAATCCGCAGC	PilU L199C F
JCP049	GCTGCGGATTTCACCAATgcAAATCATATCGGGGGCTTG	PilU L199C R
BBC2287	CATTGCGCTCGGCATTGCGTGAAGACCCAGATGTGATCtgtGTCGGTGAGCTGCGTGAC	PilT L201C F2
BBC2288	CGCAATGCCGAGCGCAATG	PilT L201C R1
BBC2369	GGCTGCCATAGTGGTCGAggcACCCGAACCGGTTGCGC	PilU K134A R1
BBC2347	GCGCAACCGGTTCGGGTgccTCGACCACTATGGCAGCC	PilU K134A F2
BBC2313	gcaggtggaagtggtggaCATCATCATCATCATCACgcaggtggagcaggtgga	6xHis (for 6xHis-PilU/T) F
BBC2314	tccacctgctccacctgcGTGATGATGATGATGATGtccaccacttccacctgc	6xHis (for 6xHis-PilU/T) R
BBC2272	gcaggtggaagtggtggagattataaagaccatgatggtgactacaaggatcacgacattgattataaggatgacgatgacaaagcaggtggagcaggtgga	3xFLAG (for 3xFLAG-PilU/T) F
BBC2273	tccacctgctccacctgctttgtcatcgtcatccttataatcaatgtcgtgatccttgtagtcaccatcatggtctttataatctccaccacttccacctgc	3xFLAG (for 3xFLAG-PilU/T) R
JCP028	tccaccacttccacctgcCATCTGTCTTTACCTACCTAAAATGC	X-PilU (N-term tags) R1

JCP029	gcaggtggagcaggtggaGAGTTGAATCAATATCTGGATGGC	X-PilU (N-term tags OR BACTH TXX-pilU) F2
JCP026	tccaccacttccacctgcCATTTAAATTCCTTAATAAAGTCTGGCTATG	X-PilT (N-term tags) R1
JCP027	gcaggtggagcaggtggaGATATCGCTGAGTTACTGGAATTTAG	X-PilT (N-term tags or BACTH TXX-pilT) F2
ABD332	GGCTGAACGTGGTTGTCGAAAATGAC	P_{tac}-PilT/U @lacZ F1
BBC244	CCCGGGATCCTGTGTGAAATTGTTATCCGC	P_{tac}-PilT/U @lacZ or @VC1807 R1
ABD255	TTAAGCTACTAAAGCGTAGTTTTCG	P_{tac}-PilT/U @lacZ F2
ABD256	CAATTTCACACAGGATCCCGGGAGGAGGTAACGTAATGGTGAGCAAAGGCGAAG	P_{tac}-PilT/U @lacZ R2
BBC1723	caatttcacacaggatcccgggAGGAGGTATTTAAATGGATATCGCTGAGTTAC	Amplify pilT (for P_{tac}-pilT) F
BBC1724	tgtaggctggagctgcttcCTAAAATGCTTTTAAATCCAACTCG	Amplify pilT (for P_{tac}-pilT OR BACTH TXX-pilT) R
BBC1725	caatttcacacaggatcccgggAGGAGGTAGACAGATGGAGTTGAATCAATATC	Amplify pilU (for P_{tac}-pilU) F
BBC1726	tgtaggctggagctgcttcCTACTCCATATCAATCTTCACATTC	Amplify pilU (for P_{tac}-pilU OR BACTH TXX-pilU) R
ABD342	ATTTTTCAGTTGGCCTACAATGCTTTCC	P_{tac}-PilT/U @VC1807 F1
BBC719	CACCATACCCACGCCGAAACAAGGATTTTGAATTAAACGTTTCATTAGTC	P_{tac}-PilT/U @VC1807 R1
BBC243	TTGTTTCGGCGTGGGTATGGTG	P_{tac}-PilT/U @VC1807 F2
BBC2667	tccaccacttccacctgcCATTACGTTACCTCCTCCCG	P_{tac}-X-PilT/U (X is 3xFLAG or 6xHis) R
BBC2513	gaagcagctccagcctacaGATCCCCGGGTACCTAAGTAAC	BACTH pKT25-X F
BBC2512	tccacctgctccacctgcCTCTAGAGTCGACCCTGCAG	BACTH pKT25-X R
BBC2515	gaagcagctccagcctacaCCGAGCTCGAATTCATCGATATAAC	BACTH pUT18C-X F
BBC2514	tccacctgctccacctgcCTCTAGAGTCGACCTGCAG	BACTH pUT18C-X R
BBC2518	gcaggtggagcaggtggaAAAGCGACCCAAACCTTACC	BACTH TXX-PilC F
BBC2524	tgtaggctggagctgcttcTTAACCCAATACACTCATTAAGTTAAAG	BACTH TXX-PilC R
BBC2358	GGTATATCTCCTTCTTAAAGTTAAACAAAATTATTTCTAGAGGGGAATTGTTATCC	pHisTev-X F
BBC2360	cggatccGGCTGCTAACAAAGCCCGAAAGGAAGCTGAGTTGGCTGCTGC	pHisTev-X R
BBC2478	TTTTGTTTAACTTTAAGAAGGAGATATACCATGgcaggtggaagtggtgga	Amplify 6xHis-pilT or 6xHis-PilU to clone into pHistev F
BBC2479	CCTTTCGGGCTTTGTTAGCAGCCggatccgCTAAAATGCTTTTAAATCCAACTCG	Amplify 6xHis-pilT to clone into pHistev R
BBC2480	CCTTTCGGGCTTTGTTAGCAGCCggatccgCTACTCCATATCAATCTTCACATTCTG	Amplify 6xHis-pilU to clone into pHistev R
BBC706	CCACACATTATACGAGCCGATG	P_{const}-tfoX R1
BBC2226	catcggctcgtataatgtgtggaGGGGAACGTGATTAAAGGA	P_{const}-tfoX F2

ABD332	GGCTGAACGTGGTTGTCGAAAATGAC	ΔlacZ::lacIq F1
ABD331	GAACATGGGGTGTACGGCAGTGCtATTTAACGATGTGCGGGTTTTGCCAATCTTG	ΔlacZ::lacIq R1
ABD255	gaagcagctccagcctacaCCACAATAAGCCAGAGAGCCTTAAG	ΔlacZ::lacIq F2
ABD256	CCCAAATACGGCAACTTGGCG	ΔlacZ::lacIq R2
ABD841	GGCACTGCCGTACACCCCATGTTCCGGTACCCGACACCATCGAATG	Amplify lacIq F
ABD842	GGCTCTCTGGCTTATTGTGGGGGGAAACCTGTCGTGCCAGCTGC	Amplify lacIq R
DOG0175	AAACTATCCAGATAAGGGAAAGC	comP (*A. baylyi*) F1
CE87	GAAGTTGTCGTACATTTCCAacaTACAGCGCCACTAGCATATG	comP T129C (*A. baylyi*) R1
CE88	CATATGCTAGTGGCGCTGTATGTTGGAAATGTACGACAACTTC	comP T129C (*A. baylyi*) F2
DOG0178	AGGATCTGTAATGACGGGTTGAG	comP (*A. baylyi*) R2
DOG0176	gtcgacggatccccggaatCATAAAATTTCTCCACCAATGTTG	ΔcomP (*A. baylyi*) R1
DOG0177	gaagcagctccagcctacaTGATAGTAGTACTATATGGCTTTAAAAG	ΔcomP (*A. baylyi*) F2
BBC1934	GTTACAAAGTCAGGGACGTAAAG	pilT or pilU (*A. baylyi*) F1
BBC1935	gtcgacggatccccggaatATCCATATTTTCCCCGAAGATCG	ΔpilT (*A. baylyi*) R1
BBC1936	gaagcagctccagcctacaTAAGAATAACGCTACTCGATCTG	ΔpilT (*A. baylyi*) F2
BBC1939	GGTATTCAGATTGATCGTCAGTTAG	pilT or pilU (*A. baylyi*) R2
BBC1937	gtcgacggatccccggaatCATCGTATTGTTTTCCTCTCAGATC	ΔpilU (*A. baylyi*) R1
BBC1938	gaagcagctccagcctacaCGCCGTAATCTCAAATAAAAGAG	ΔpilU (*A. baylyi*) F2
BBC2403	GCTGCAAGGGTGGTTGAagcACCGGAACCAGTGG	pilT^{K136A} (*A. baylyi*) R1
BBC2404	CCACTGGTTCCGGTgctTCAACCACCCTTGCAGC	pilT^{K136A} (*A. baylyi*) F2
BBC2408	GGATGCCAAAGACGTGGAagcTCCTGTACCAGTTGC	pilU^{K137A} (*A. baylyi*) R1
BBC2409	GCAACTGGTACAGGAgctTCCACGTCTTTGGCATCC	pilU^{K137A} (*A. baylyi*) F2
BBC2807	caatttcacacaggatcccgggAGGAGGTGAAAATATGGATATAACAGAATTACTCG	pilT amplify for insertion into P_{tac} construct (*A. baylyi*) F
BBC2808	tgtaggctggagctgcttcTTAGAACGACTCTGGAGATTTTG	pilT amplify for insertion into P_{tac} construct or pMMB67EH (*A. baylyi*) R
BBC2809	caatttcacacaggatcccgggAGGAGGTAATACGATGGACTTTAATGATTTACTC	pilU amplify for insertion into P_{tac} construct (*A. baylyi*) F
BBC2810	tgtaggctggagctgcttcTTATTTGAGATTACGGCGTTGAC	pilU amplify for insertion into P_{tac} construct or pMMB67EH (*A. baylyi*) R

BBC2822	aatttcacacaggaaacagaattcgagctcTTGTTTCGGCGTGGGTATGGTG	Clone P_{tac}-pilT or P_{tac}-PilU into pMMB67EH (*A. baylyi*) F
BBC2824	gagctcgaattctgtttcctgtgtgaaattTTTGCCAGAACCGTTATGATGTC	Amplify pMMB67EH to clone P_{tac}-pilT or P_{tac}-pilU (*A. baylyi*) F
BBC2357	GGTACCCGGGGATCCTCTAGAGTCGACCTGCAGGCATGCAAGCTTGGC	Amplify pMMB67EH to clone P_{tac}-pilT or P_{tac}-pilU (*A. baylyi*) R